Fuel 254 (2019) 115646

Contents lists available at ScienceDirect

Fuel

journal homepage: www.elsevier.com/locate/fuel

Review article

On the combustion of heterogeneous AP/HTPB composite propellants: A review

Claresta Dennis, Brian Bojko*

Combustion Science and Propulsion Research, Naval Air Warfare Center Weapons Division, China Lake, CA 93555, USA

ARTICLE INFO

Keywords:
Solid propellant
Burning rate
AP
HTPB
Heterogeneous combustion

ABSTRACT

The combustion of ammonium perchlorate (AP) in a polymer binder matrix of hydroxyl-terminated-polybutadiene (HTPB) is reviewed, covering the experimental and modeling approaches explored for over a half-century. AP is capable of self-deflagration and is a propellant in its own right as ammonia and perchloric acid decompose at the surface to sustain a flame in the gas-phase with an adiabatic flame temperature of roughly 1400 K. AP also has unique low temperature decomposition behavior and burning characteristics as a function of pressure attributed to the importance of condensed phase reactions. A polymer, most commonly HTPB, is used to bind AP crystals within a solid matrix and impart desired mechanical properties and additional fuel for inclusion in a solid rocket motor. Aside from providing an additional fuel source for the decomposing AP, the HTPB introduces diffusion flames into the system, which have the advantage of decreasing the combustion instability of the AP monopropellant. The objective of this paper is to review the critical physical processes of AP/HTPB propellant combustion and to explore the different experimental and computational avenues used to shed light on such a complex phenomenon. Experimental diagnostics and the simulation of solid propellant combustion have progressed immensely over the years with the introduction of more advanced laser diagnostics and imaging techniques, as well as an increase in computational resources and processing power available for computations; additional physics can now be modeled that would have otherwise been impossible to include before. A recommendation on future research is given based on the current state of the art.

1. Introduction

This paper is a review of the experimental and computational methods used to study the combustion of a heterogeneous solid propellant using ammonium perchlorate (AP) as the oxidizer in a hydroxyl-terminated polybutadiene (HTPB) fuel. The study is organized as follows. Firstly, the important physiochemical processes of AP/HTPB combustion are presented with detail provided on each process to provide an overall picture on the complex multi-phase burning event. Next, the experimental diagnostics that have been applied to study each of these processes are presented. Then a summary of the modeling and simulation of AP monopropellant flames and the composite system are presented with discussion of the various methods used. Finally, conclusions are drawn on the current understanding of AP/HTPB burning and suggestions are made for future improvements in diagnostics and modeling.

1.1. Physiochemical processes occurring during AP/HTPB propellant combustion

Composite propellant burning is viewed as a multi-step process:

- First, the endothermic decomposition of the solid oxidizer and fuel
- Second, the exothermic condensed-phase reactions (AP decomposition)
- Third, the exothermic premixed reaction of $NH_3/HClO_4$ with condensed-phase reaction products (AP monopropellant flame)
- Fourth, the exothermic fuel-oxidant reaction (primary diffusion flame)
- Fifth, the diffusional mixing and chemical reaction processes in the O/F flame zone (final diffusion flame)

Based on review of the literature, including experimental and theoretical work, a schematic of the AP/HTPB propellant combustion process at atmospheric pressure was created. The propellant grain was digitized from an actual 88% solids loading propellant with a trimodal

* Corresponding author.
E-mail address: brian.bojko@navy.mil (B. Bojko).

https://doi.org/10.1016/j.fuel.2019.115646
Received 10 April 2019; Received in revised form 10 June 2019; Accepted 11 June 2019
Available online 21 June 2019
0016-2361/ Published by Elsevier Ltd.

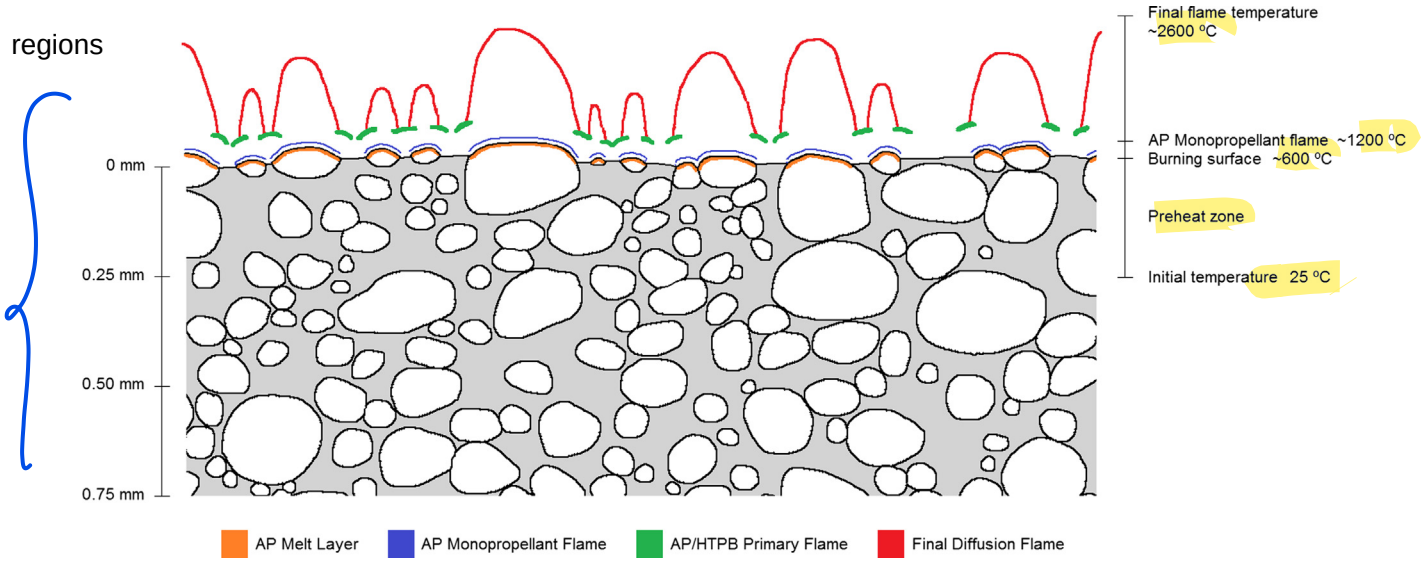

Fig. 1. Schematic of AP/HTPB propellant combustion at atmospheric pressure.

distribution of AP particles. Features are approximately to scale and it is important to note that diffusion flame structure depends on initial propellant conditions and ambient conditions during burning. Based on experimental species concentration measurements, the reactions zones are distributed and the typical flame sheet analysis as shown here is only approximately correct [1]. Multimodal propellants are also more difficult to illustrate due to flame interactions. Particles have different reaction rates due to relative strength of the monopropellant and primary flames and proximity to final diffusion flames [2]. In addition, the reaction zone distance is a function of particle size and the flames above very small AP particles are premixed.

Fig. 1 does illustrate length scales, providing insight as to the difficulty of obtaining experimental validation of multiphase chemistry occurring over a few thousand degrees in less than 1 mm. As pressure increases to levels significant for rocket motor applications, the AP melt layer becomes even thinner, AP monopropellant flame thickness is negligible, the primary flame zone sits much closer to the surface and is rate controlling.

1.2. Conductive heat feedback to the regressing surface, pre-heating "thermal wave"

Heat feedback to the regressing surface from the adjacent exothermic gas-phase reaction zone is the main energy flux driving the "thermal wave" in a solid propellant [3]. The term thermal wave is used to refer to the spatial temperature profile established within the subsurface of a burning solid propellant due to diffusion from its time varying heat source. Energy arriving at the propellant surface by conductive heat feedback is used to heat the solid from its initial temperature to the surface temperature and also to gasify the condensed-phase propellant constituents.

Experimental measurements of the thermal wave have been reported based on embedded micro-thermocouples [4–7]. This technique draws criticism due to high uncertainties in position and the heat transfer corrections required [8]. Measurements show that the depth at which the bulk solid is preheated is on the order of 50–200 μm [4].

A key boundary condition in the thermal wave is the temperature of the burning surface. This boundary condition, when given as a function of the mass regression rate, can be used to characterize condensed-phase kinetics [9]. Attempts to measure the burning propellant surface temperature, either by embedded micro-thermocouples, radiation measurements, or calorimetry, give values between 670 and 973 K [10]. Beckstead et al. [11] burned large single AP crystals at pressures up to 74.9 atm, extinguished the samples, and observed changes using polarized microscopy. Evidence of a thin melt layer approximately 2–3 μm thick was apparent and the surface temperature of burning AP was determined to be 833 K.

1.3. AP decomposition

The thermal decomposition of ammonium perchlorate includes multiple chemical and physical processes and is often categorized by low and high temperature decomposition regimes. Many studies have demonstrated a dependence of reaction product composition and extent of degradation on temperature [12,13]. Low temperature decomposition has been demonstrated to occur between 473 and 573 K at atmospheric pressure and is associated with the production of Cl_2, H_2O, N_2O, O_2, ClO_2, HCl, N_2, NO, NO_2Cl and other nitrous gases. High temperature decomposition occurs above 653 K and is associated with the production of H_2O, ClO_2, Cl_2, O_2, NO, NO_2, N_2O_3, N_2O_4, $NOCl$, $HClO_4$. Deflagration begins at ~708 K and its onset is pressure dependent. At 513 K, ammonium perchlorate undergoes a crystalline phase transition from an orthorhombic to a cubic form. The degradation process begins with dissociative sublimation of the NH_3: $HClO_4$ complex by proton transfer to produce ammonia and perchloric acid at the crystal surface [12]. The solid-to-gas phase transition does not take place uniformly throughout the AP crystal, it spreads hemi-spherically outwards from certain nucleation sites [3]. The formation, growth, and migration of these pores has been recently quantified by nano-computed tomographic measurements during isothermal heating [14]. The activation energy for the dissociative sublimation step of commercial grade AP was found to be 30 kcal/mole whereas the value for highly purified AP is around 100 kcal/mole. Acceleration of decomposition has been observed due to impurities forming nucleation sites, lattice dislocations induced by radiation, partial deuteration, and doping with foreign ions [15–17]. During the degradation process, approximately 30% of the AP experiences sublimation and vaporizes, while the remaining 70% decomposes at the surface through exothermic condensed-phase reactions [18–20].

The combination of gas and condensed-phase heat release are responsible for AP decomposition at varying levels for a range of pressures. However, gas-phase reactions alone cannot be used to describe the decomposition process of AP at all pressures [21,22], especially above 136 atm, thus emphasizing the importance of the condensed phase and exothermic heat release as a rate controlling process of the AP decomposition. The solubility difference between perchloric acid

and ammonia vapors along with the formation of intermediate products within the condensed-phase can explain a drop in AP burning rate with pressure and combustion instability above 136 atm [19]. The competition between sublimation and condensed-phase decomposition can only be accurately accounted for by models, which include condensed-phase chemistry; a requirement for accurate solid composite burning rate modeling.

In a burning solid composite propellant AP has a very thin melt layer, at most a few microns thick. Evidence of a melt layer has been observed experimentally; Boggs and Hightower found entrapped gas bubbles and surface patterns of troughs and ridges on the surface of quenched AP [23,24]. Theoretical work has determined the melting temperature of AP to be approximately 835 K [18]. Whether this layer is mobile or immobile during propellant combustion depends on AP content and particle size; a mobile melt layer has been shown to result in unsteady propellant burning behavior [3]. Although the decomposition of AP in pressure ranges from 7.1 to 143 atm can be mostly attributed to the sublimation to $NH_3 + HCLO_4$ with few condensed-phase contributions, a detailed mechanism of the decomposition and combustion of AP remains undefined for the entire pressure range relevant to rocket motor environments. Further research is necessary to better understand the condensed-phase reaction process, AP decomposition, and heat release occurring during this stage.

1.4. Binder melting/decomposition

The chemistry of HTPB polymer decomposition is extremely complicated. The mechanism of pyrolysis involves random scission and/or systematic unzipping of the polymer chain to produce a gaseous mixture of monomer units and chain fragments of varying sizes [3]. Above 773 K, the cracking of large chains becomes important and monomer yield is reduced. Assumptions that a propellant binder decomposes into monomer type fragments, such as butadiene for which the combustion mechanism is known, without taking into account the detailed polymer breakup chemistry, are not appropriate [1]. In addition, as pressure increases, monomer yield is reduced and the proportion of dimers, trimers, etc. are increased. Extrapolating bulk degradation kinetic data to the temperature and pressure conditions typically encountered in a solid rocket motor should be avoided. Chen and McQuaid [25 26] used quantum chemistry and group additivity techniques to develop reaction pathways for the pyrolysis and combustion of HTPB that include large hydrocarbon molecules with up to 20 carbon atoms in order to include the larger molecules that form due to cyclization, isomerization, and β-scission. In addition to the complex breakup chemistry of the long-chain hydrocarbons, different plasticizers, curing agents, catalysts, antioxidants, etc. are also used in the binder formulation and can have a significant impact on the burning rate. Miller et al. [27] studied the effects of two different curative agents, isophorone-diisocyanate (IPDI) and dymeril-diisocyanate (DDI), and typically found an overall increase in burn-rate with IPDI. Chen and Brill [28] also investigated the pyrolysis kinetics of pure HTPB compared with HTPB with different diisocyanate cross-linking agents, such as toluene diisocyanate (TDI), IPDI, and DDI. They found a range of regression rates between, 0.09 to 0.21 mm/s from the pure HTPB to HTPB-IPDI, respectively.

A binder pyrolysis study was performed by Cohen et al. [29] on HTPB up to 17.0 atm with a radiant flux of 300 cal/cm^2-s and up to 68.0 atm at 50 cal/cm^2-s. They found HTPB to exhibit a boiling surface and carbonaceous char, which increases with pressure and chlorine addition, indicating thermal and oxidative degradation and gas-phase reactions. A weak-link degradation mechanism or physical boiling process describes the degradation observed, not molecular bond rupture. HTPB degradation investigated using gas chromatography has shown at 1169 K butadiene accounts for only 1–2% of the products, and the primary product is ethylene [30]. In search of a mechanism for HTPB degradation in the presence of AP decomposition products, Didikin et al. [31] performed detailed measurements on the oxidative destruction of rubber films exposed to $HClO_4$ vapor. They found the rate of reaction is related to reaction extent, film thickness, $HClO_4$ partial pressure, and temperature.

1.5. AP monopropellant flame – $NH_3/HClO_4$

The AP "monopropellant flame" consists of the exothermic redox reaction between gases produced by the dissociative sublimation of AP to NH_3 and $HClO_4$. The monopropellant flame is modeled as a premixed flame, and its experimentally determined low-pressure limit is ~20 atm [32,33]. Experiments have shown the AP surface recedes below the propellant binder surface at high pressures, suggesting that the monopropellant flame has a controlling influence on the burning rate in the very high pressure range, > ~100 atm.

1.6. Primary diffusion flame – AP/HTPB

The "primary diffusion flame" is located at binder/oxidizer boundaries, occurring between HTPB pyrolysis products and oxidant resulting from the AP monopropellant flame. Due to the heterogeneous nature of composite propellants the fuel and oxidizer gases are unmixed as they emerge from the propellant surface, thus rates of diffusional mixing and chemical reaction determine the overall reaction rate of the primary flame [3]. There is a range of pressures where the AP monopropellant flame and the primary flame are competing for the reactive oxidizer species. At typical rocket motor pressures, ~68.0 atm, the primary flame extends approximately 20 μm from the regressing propellant surface and acts as the rate controlling flame [1,34].

1.7. Final diffusion flame

A "final diffusion flame" is present where the slowest reactions (such as $NO \rightarrow N_2$ and $CO \rightarrow CO_2$) are completed [1]. This includes any subsequent reactions between product gases of the AP monopropellant flame and the primary diffusion flame and any remaining fuel pyrolysis products. The final oxidizer-fuel flame is positioned within a distance of about 100 μm from the regressing propellant surface at elevated pressure [3] and is thought to have a limited impact on the heat feedback to the surface.

1.8. Pressure dependence

The chemical properties, such as decomposition and oxidation, and physical parameters, such as heat and mass transfer in three dimensions, determine how the propellant combustion will progress and be affected by external conditions. The relationship between the various length scales, AP particle size, interstitial particle distances, and reaction zone thickness, gives rise to complex burning rate and pressure dependences [35,36]. Many researchers over the years have observed pressure effects during the combustion of AP/HTPB based composite propellants; AP particles appear to protrude from the burning surface at low pressures and form cavities or depressions beneath the surface at high pressures [37]. In general, the relationship between solid composite propellant burning rate and ambient pressure at the surface follows a power law as shown in Eq. (1), where r_b is the burning rate and P is pressure. Typical pressure exponents, n values, are between 0.2 and 0.7.

$$r_b = aP^n \tag{1}$$

Propellants and solid rocket motors (SRMs) are designed to operate at pressures between 47.6 and 102 atm, though composite case technology has enabled higher operating pressures above 136 atm. At these elevated pressures the burning rate trends change, computational models have been created which seem to capture the burning behavior well at one pressure regime and not at others. The main source for these difficulties is the unique relationship between AP deflagration and

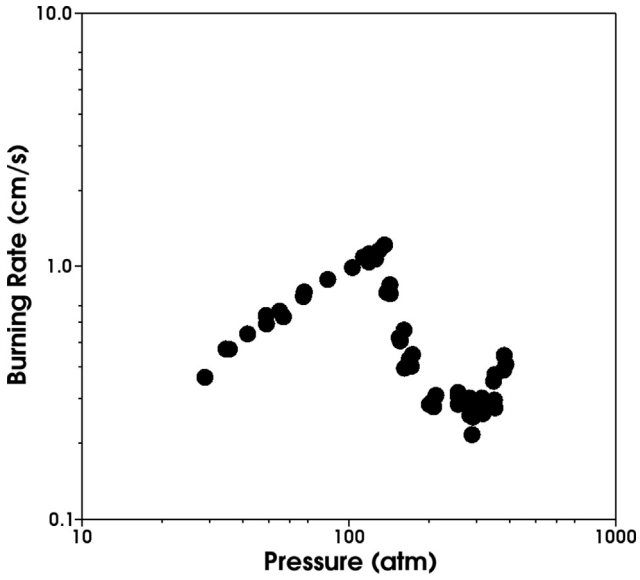

Fig. 2. Burning rate vs pressure for ultra-high purity AP at ambient temperature from Atwood et al. [33]

pressure.

Four pressure regimes for the deflagration of AP were defined by Boggs and Kraeutle [32] and have since been observed by many others. The location of the regimes does depend on the initial temperature of the AP samples [19]. Atwood et al. [33] investigated the burning rate dependence as a function of initial temperature and at varying pressures for a variety of energetic materials used in propellants, including AP. The AP samples used included high purity single crystals and pressed pellets (over 99% TMD); no difference in burning rate was found between the single crystals and pellets as long as high purity AP was used. An increase in burn-rate was observed with an increasing initial temperature from, $T = 298 - 423$ K, as well as an increase in temperature sensitivity, σ_p. They found the low-pressure deflagration limit for pure AP at ambient temperature is approximately 19.7 atm, which is reproduced in Fig. 2. In 'Region 1', between 19.7 and 61.2 atm, there is a positive exponential burning rate dependence with pressure and evidence that gas is liberated from the solid AP surface and travels up through a liquid melt layer. This liquid layer thickness decreases with increasing pressure. In 'Region 2', between 68.0 and 136 atm, the burning rate dependence has a decreasing positive slope with its exponent approaching zero. In 'Region 3', between 136 and 272 atm, the burning rate slope is negative, combustion is not stable, appears to pulsate, and does not progress uniformly over the surface. In 'Region 4', above 272 atm, they found combustion becomes more stable as gas-phase reactions dominate and the burning rate curve takes on a high positive pressure exponent. In a composite propellant, these pressure regions give rise to "slope breaks" in the burning rate curves.

Experimental measurements at elevated pressure conditions are difficult. The premixed flame zone is drawn closer to the propellant surface as the final diffusion flame moves farther from the surface. Gas properties such as transport or diffusivity of combustion product gases are not well understood. Optical diagnostics are difficult due to sharp density gradients in the flow, requirements for thick windowed combustion bombs, and spectroscopic line broadening and mixing. Furthermore, large AP crystals will crack at elevated pressures increasing the surface area and increasing the uncertainty of burn-rate measurements.

1.9. Particle size dependence

In addition to the pressure dependence on the burn-rate, when AP is bound within a polymer matrix, it also exhibits a size dependence on the flame shape and burn-rate. As the particle size decreases from larger, ~400 μm, to smaller ~1 μm AP crystals, the flame transitions from a diffusion to a premixed regime. Gross and Beckstead [38] showed this numerically, simulating the combustion of a single AP particle within HTPB at an overall solids loading of 86%. Detailed gas-phase combustion chemistry is employed in the simulation and the flame shape can be clearly seen to detach from the surface and hover over the propellant as the particle size decreases, as seen Fig. 3. At small particle sizes, the burn-rate of the propellant is governed by the premixed limit and at larger AP sizes, the burn-rate is limited by the deflagration of AP.

The stoichiometry, and temperature, of diffusion flames occurring above AP in a burning composite propellant are particle size dependent; small AP particles tend to burn fuel rich while larger particles burn fuel lean. Experimental work has demonstrated the relationship between AP particle size and burning rate as a function of pressure and solids loading percentage, the most comprehensive performed by Miller and Foster [39,40]. Particle size has a significant effect on burning rate due to this change in stoichiometry and diffusional length scales [34]. For example very fine AP (< 12 μm diameter) can react with HTPB in a

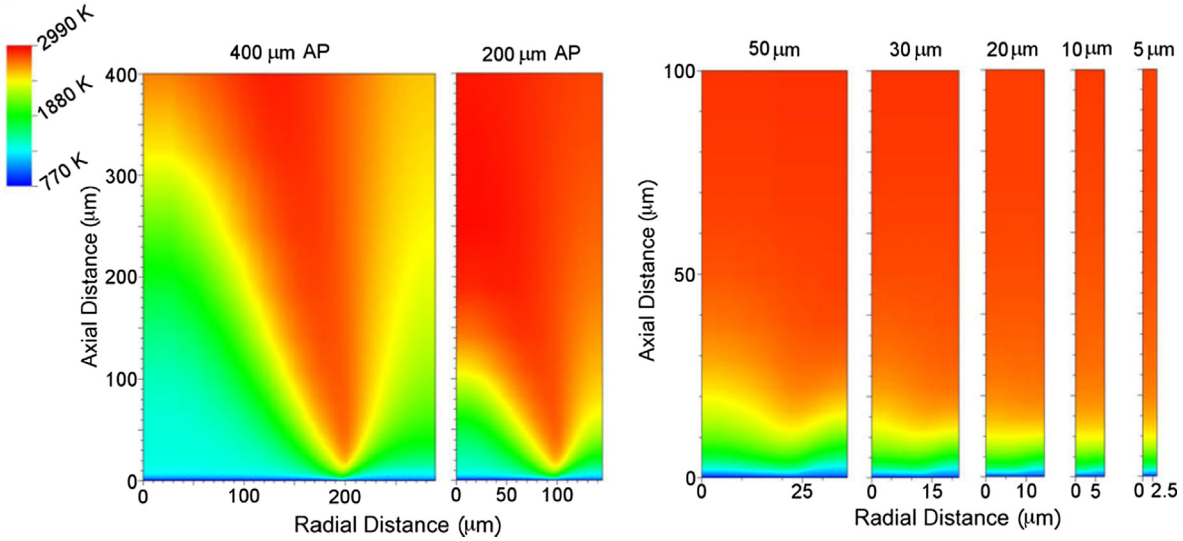

Fig. 3. Flame shape of single AP particles burning in an HTPB binder with detailed chemistry varying the particle size from 400 to 5 μm. This figure is reproduced from Gross and Beckstead [38].

premixed flame, intermediate sized AP (~20 to 80 μm) will produce competing flames, and for large particle sizes (> 90 μm) the AP monopropellant flame dominates. A distribution of different particle sizes is included in propellant formulations to control burning rate and achieve desired solids loading based on propulsive requirements. In general, a decrease in AP particle size will increase propellant burn-rate however due to the increased surface area of very fine particles achieving a homogenized propellant mix with appropriate mechanical properties, i.e. pourable for casting, is challenging. The combination of pressure and size dependencies on the burn-rate is a unique feature of propellants containing ammonium perchlorate, and is highly advantageous when designing propellants for a variety of rocket applications or even for different burn-rates within a single motor to optimize its ballistic performance.

1.10. Burn-rate measurements

Burning rate is the most important property of a solid composite propellant for use in propulsion applications. Many different measurement techniques are used, each with its own associated advantages and limitations. In 1996, the NATO Research and Technology Organization – Advanced Vehicle Technology, established a working group to evaluate the various methods used to measure burning rate in solid propellant rocket systems. A final report was completed with recommendations based on direct and non-intrusive measurement methods, data analysis, and performance scaling to support full-scale rocket motor ballistics predictions [41]. Lab-scale strand burner experiments are preferred for assessing statistically significant effects of propellant formulation changes and validation of modeling and simulation efforts. However, in general full-scale motors, sub-scale motors, and propellant strands do not have the same burning rate at the same pressure and a correlation or scale factor is used to relate them.

In the laboratory setting, the most common setup for burn-rate measurements is the strand burner. The Crawford type strand burning rate bomb is the standard measurement for assessing rocket propellant performance and is detailed in MIL-STD-286C [42]. The stainless steel bomb is 60 in^3 in volume with a 340.2 atm working pressure. Propellant samples are coated in epoxy inhibitor, prepared with ignitor and timing wires, and loaded into the bomb fixture. As the strand ignites and burns, gas is exhausted to maintain the original pressure. Time of burning between two fusing wires is recorded, converted to burning rate, and plotted as a function of pressure. The main requirement for strand burner measurements is one-dimensional burning; proper care must be taken to inhibit propellant sides from burning.

The Closed Bomb is a variation in which the pressure is allowed to build up during combustion and pressure variation is measured as a function of time. Burn-rate is then based on equilibrium thermochemistry and calculations require specific heat and heat of combustion. Typically, closed bombs are used for assessing changes in burn area, such as friability, on materials designed to operate at higher pressures than standard rocket motors.

Window bombs, operated in either a pressure controlled or closed bomb fashion, for propellant strand burning enable the ability to employ optical diagnostics and obtain additional information about the ignition and combustion processes. Various window materials are used based on transparency at wavelengths of interest. Burn-rate measurements in window bombs may then be based on cinephotomicroscopy where high-speed video images are used to track burning surface regression; such measurements historically are associated with ~3% uncertainty.

The most accurate method for burn-rate determination is ultrasonically. Propellant is attached to a coupling material with a transducer. Mechanical waves travel through the sample and are reflected at the burning surface back to the transducer. These measurements are associated with uncertainty as low as 1% [41].

Aside from propellant performance, burn-rate measurements have been a key component for model validation, using idealized sandwich propellants and strand burner data. Miller et al. [43–45] created ~25 different propellant formulations at a variety of size distributions of AP from 3 to 400 μm and with a solids loading of 87.4% and measured their average burn-rates. These studies were used to determine the influence of fine AP in a distribution and the effect of the width of the AP distribution on the burning rate as a function of pressure. Foster and Miller [46] updated this database to also study the effects on the temperature sensitivity, σ_p, and observed wide AP distributions at a constant burn-rate increase the temperature sensitivity by nearly 200%. Price et al. [47,48] used quenched AP/HTPB sandwich propellants to give a qualitative analysis of the burning surface using SEM to study the microstructure of the surface. Lee et al. [49] also looked at sandwich propellants to describe the canopy flame structure and the importance of kinetic to diffusion-controlled combustion from low to high pressures, respectively.

2. Experimental diagnostics

Many efforts have been made over the years to understand and validate the physiochemical processes, which occur during solid composite propellant combustion. Edwards published a review in 1988 [1] of the various diagnostic techniques and the measurements they provided. Over the last 30 years, research has continued and advances in technology enabled measurements not previously possible. The various techniques are discussed with respect to work published since the review by Edwards. While the focus of this review is on the combustion of AP/HTPB composite propellants, experimental diagnostics demonstrated on other propellant systems may also be useful and those examples are addressed.

2.1. Mass spectrometry (MS)

Mass spectrometry (MS) is a common analytical chemistry technique for species detection and identification based on the molecular weights of molecules within a sample. Samples are ionized and the isotopic signature is observed as a function of the mass-to-charge ratio. There are now many variations on the technique, each optimized for the sample under evaluation. Molecular beam mass spectrometry (MBMS) has been used to trace various chemical species in stationary combustion processes; gases are probed in-situ and the sample is expanded into a molecular beam. Chemical reactions are quenched immediately and the sample composition is considered “frozen”, so highly reactive species, such as radicals, can be preserved and detected by this technique. For combustion diagnostics, MBMS is often coupled with a high temperature flow reactor to validate gas-phase reaction kinetics.

The majority of mass spectrometry research applied to AP/HTPB composite propellant was performed by Korobeinichev et al. in the early 1990s [50–52]. Efforts were made to improve the sampling method and spatial resolution for measurements on AP, AP simulant flames, AP in binders, and AP with a catalyst; still there were difficulties noted in flames with narrow combustion zones. They reported 15% error in concentration measurements and 30% error in combustion zone width. Measurements confirmed that 20–30% of AP decomposes in the condensed state to give the final products HCl, Cl_2, N_2, N_2O, NO, etc., while 70–80% produces intermediates ClO_2, $ClOH$ and products from dissociative sublimation NH_3, $HClO_4$ which react further in the flame. Sub-atmospheric pressure, ~0.5 atm, measurements during the combustion of an uncured composite containing 77% of 200 μm AP particles and 23% HTPB was used for the basis of a chemical reaction mechanism [51]. Seven stable components in the flame zone were detected.

The experiment was repeated at 0.08 atm using 50 μm AP and they found the different flame structures could not be described with the same collection of rate constants suggesting a change in reaction mechanism with low pressure [52].

More recently Volkov et al. [53] applied MBMS to RDX (1,3,5-Trinitro-1,3,5-triazinane) combustion at atmospheric pressure and identified RDX vapor and 10 additional species. Two distinct chemical reaction zones were identified and a global reaction mechanism was presented. While mass spectrometry has been used for the majority of AP/HTPB reaction mechanism development work, the technique draws criticism due to its limited spatial resolution, requirement for a gas sampling probe, which introduces a physical disturbance to the flame, and the technique may produce skewed results due to radical recombination and quenching.

2.2. Chemiluminescence imaging

Chemiluminescence imaging is one of the most widely used optical diagnostic techniques for combustion. Chemical reactions in the flame front create regions of high local heat release, species are excited and emit light. The most commonly imaged species is the intermediate *OH* as it is formed in the flame front of hydrocarbon oxidation. High-speed cameras and intensifiers have made this technique applicable for fundamental turbulence/chemistry interaction studies.

Chorpening et al. [54] studied the combustion of AP/HTPB laminates using *OH* chemiluminescence, consisting of a 50 to 450 μm thick layer of HTPB sandwiched between AP at ambient pressures between 2 and 31 atm. Fitzgerald and Brewster [55,56] also applied chemiluminescence imaging laminates. They imaged *OH* and *HCl* with spectral filters at 310 and 3520 nm respectively. Their experiments were performed up to 50 atm. They found at relatively low pressures (< 15 atm), imaging shows two stream-wise distinct diffusion flames, which are possibly the primary diffusion flame and final diffusion flames. As pressure increases the two flames appear to merge streamwise and become indistinguishable, as the final diffusion flame moves closer to the surface to merge with the primary diffusion flame to create a continuous reaction zone. Results highlight the importance of the primary flame, occasionally referred to as the “leading edge” flame, which involves reactions between the AP and binder decomposition products. Although, *OH* is the most common species targeted, the *OH* radical signal is affected by reabsorption and is best suited for diagnostics of systems of low optical thickness, not necessarily propellant combustion.

2.3. Thermocouples

Thermocouples have been employed since the earliest propellant studies, typically embedded within a propellant strand which then emerges to the surface during burning and temperature is recorded as a function of distance above the propellant surface. High temperature platinum type thermocouples are preferred and the wire should be 0.3 mm or finer for a bead diameter less than 0.5 mm. Jojic and Brewster [57] used thermocouples to investigate condensed-phase reactions between AP and HTPB. Thin films of 2 μm AP and HTPB were prepared on a glass slide for CO_2 laser ignition and a micro-thermocouple was embedded within the sample to record the thermal response. A strong condensed-phase chemical interaction was found to occur between fine AP and HTPB as had been previously reported for similar polymers under slow heating conditions.

Optical methods are preferred over thermocouples to eliminate the physical intrusive probe, limited spatial resolution, and issues with survivability of the sensor.

2.4. UV/VIS/IR emission spectroscopy

Emission spectroscopy is used for species identification and temperature measurements and has been applied to propellant combustion in the ultraviolet, visible, and infrared regions of the electromagnetic spectrum. Weiser et al. [58] studied the combustion of ADN (ammonium dinitramide)/paraffin strands from 4.93 to 98.7 atm. They observed emissions from OH, NH, CN, H_2O, CO_2, CO, NO, and HCl and used the OH emission to obtain a rotational temperature of 2700 K. Yang et al. [59] performed experiments on a composite propellant containing 16.5% HTPB, 68% AP, and 14% Al at 29.6, 49.3, and 69.1 atm. They made radial spectral scans to obtain flame temperature distributions at various distances above the propellant surface. Temperatures were calculated from relative emission intensities of three nitrogen (II) ion lines. Disadvantages of the emission spectroscopy technique are that it is line of sight, path averaged, it is difficult to get measurements with high spatial resolution, and resulting spectra can be complicated to analyze. Further, temperature measurements obtained from spontaneous emission assume thermal equilibrium given by a Boltzmann distribution of populated states [60]. Spectral emissions are proportional to the concentration of chemically excited states of a species resulting in measurement bias towards high temperatures.

2.5. Absorption spectroscopy

Absorption spectroscopy measures the absorption of radiation due to its interaction with a sample and is often used for remote sensing applications and species concentration measurements. For combustion diagnostics these experiments have been performed with coherent and incoherent light. One of the main difficulties is distinguishing the input signal from the luminosity produced by the reaction.

Nitramine combustion has been studied using absorption spectroscopy as the flames are clean, containing little to no obscurant. Homan and Vanderhoff [61] performed absorption spectroscopy on neat RDX monopropellant to obtain CN and NH species concentrations using a 150 W pulsed arc lamp. In order to study condensed-phase processes in nitramine propellant combustion a novel approach was taken by Wormhoudt et al. [62] in which IR absorption spectroscopy was applied within a propellant sample. Fiber optic was inserted into a small hole within a propellant sample, leaving a 0.2 to 0.5 cm air gap as the sensing region. This cavity filled with gas-phase decomposition products as the flame front approached. Their results support that N_2O originates in pressurized bubbles inside liquid RDX.

Lu et al. [63] applied absorption spectroscopy in the 307–311 nm region to measure flame temperature and OH concentrations of a double-base propellant at pressures up to 69.1 atm. While flame temperatures obtained at high pressure agreed well with chemical equilibrium calculations, measured OH concentrations were 40% lower than calculated. They attribute the discrepancy to the high sensitivity of OH concentration to variations in local flame stoichiometry and temperature.

2.6. Fourier-transform infrared spectroscopy (FTIR)

Most experiments which have applied FTIR to study propellant combustion rely on rapid thermolysis of the sample and analyzing the gaseous decomposition products which evolve [64]. FTIR absorption measurements for speciation have the advantage of not being complicated by fluorescence lifetime effects or pre-dissociation. A unique approach by Li and Wang [65] used a remote sensing FTIR spectrometer and telescope attachment to collect the IR emission during combustion of a nitroguanidine/AP/PTFE (polytetrafluoroethylene) solid propellant from 30 m away. They obtained spectra between 800 and 4700 cm^{-1} which enabled temperature determination from the ro-vibrational bands of HF and HCl. Commercially available FTIR instruments are expensive, have limited temporal resolution, and the measurements are line-of-sight and path averaged. In addition, large molecules can produce FTIR spectra with overlapping bands, making species identification uncertain.

2.7. Laser based spectroscopic techniques

Non-intrusive laser-based spectroscopic techniques are preferred for

the experimental determination of temperature and molecular species concentrations, flow-field characterization, and turbulence-chemistry interactions. Several techniques and their variations have been applied to better understand the combustion processes of solid composite propellants.

2.7.1. Planar laser-induced fluorescence (PLIF)

PLIF is a spectroscopic technique for species detection, temperature measurements, and flow visualization. An atom or molecular species is excited with a laser then after some time it will relax and spontaneously emit or fluoresce light at a longer wavelength which is detected. PLIF is used for combustion diagnostics because it is non-intrusive to the flow and helpful to quantify combustion progress species such as OH.

Smooke et al. [66] applied diagnostics to an AP/ethylene counterflow flame at atmospheric pressure for study both experimentally and computationally. For temperature measurements they used thermocouples, OH rotational spectra, and NO vibrational absorption spectra. Species concentrations of OH, CN, NO, and polycyclic aromatic hydrocarbons were obtained using 10 Hz PLIF. Soot volume fraction was measured using laser induced incandescence. They observed four distinct flame regions: the AP monopropellant flame ~50 μm from surface, a light blue region where OH begins to appear, a red-purple colored region containing the primary diffusion flame with high radical concentrations, and finally a bright yellow region with soot. Most surface oxy-chlorine compounds, ClO_2 and $HClO_4$, were found to disappear within 0.1–0.2 mm of the AP surface.

Advances in solid-state laser technology have enabled the commercial availability of very high repetition rate laser systems and ability to perform kHz repetition rate PLIF. Hedman et al. [67] used 5 kHz OH PLIF for studying AP/HTPB composite propellant combustion at atmospheric pressure. Two propellant formulations with 80% solids loading were studied to observe particle size dependences. With the OH signal they determined single particle ignition delay and burning time. They observed AP fluoresces when irradiated with 283.2 nm laser light. More recently, Isert et al. [2] applied 5 kHz OH PLIF to several unimodal AP/HTPB propellants and AP pellets containing HTPB filled holes at atmospheric pressure. For propellants with AP sizes of 24, 46, and 137 μm only a haze of OH is seen above the propellant surface. Propellants prepared with 230, 450, and 797 μm AP show clear flame structures above each individual particle.

Laser induced fluorescence measurements are difficult to make quantitative, requiring at least two spectroscopic lines to determine temperature. Edwards [1] recommends NO LIF for temperature measurements of propellant flames at elevated pressure rather than OH LIF due to the rovibrational structure. For LIF of a diatomic molecule, one should consider the vibrational and rotational structure and the potential for photoionization to the continuum and predissociation [60]. Signal-to-noise ratio is limited by detector shot noise; signals can be quite low requiring the use of intensifiers and self-quenching of the signal can occur due to the line-of-sight nature. There can be fluorescence interferences from other species present, especially from hydrocarbons in high pressure reacting flows, and beam attenuation due to scattering from particles in the flow.

2.7.2. Spontaneous Raman scattering (SRS)

Raman scattering is the inelastic scattering of light by excited molecules; molecules either absorb energy and the emitted photon has a lower energy or the molecules lose energy and the emitted photon has a higher energy. The resulting Raman spectrum shows the intensity of scattered light as a function of its frequency difference with the incident photons and depends on the populations of the initial states of the molecules. The major difference between fluorescence and SRS is that the Raman effect can take place for any frequency of incident laser light, SRS is not a resonant effect. This is advantageous as it allows the detection of many Raman active species using only a single excitation wavelength.

The Parrs [68] used SRS and other non-intrusive techniques, PLIF and UV/VIS absorption spectroscopy, to determine species and temperature profiles above the surface of self- deflagrating RDX/GAP (glycidyl azide polymer)/BTTN (1,2,4-Butanetriol trinitrate) propellant at atmospheric pressure. Major species detected near the surface were HCN, CO, and N_2 and the burnt gases contained CO, N_2, H_2O. They observed a dark zone where NO concentration was at its highest. The experiment was repeated using HMX (1,3,5,7-Tetranitro-1,3,5,7-tetrazoctane)/GAP/BTTN propellant [69]. At the surface the major species were CO, H_2O, NO_2, N_2O, and H_2CO, in the dark zone species were NO, CO, H_2O, and HCN, and finally the burnt gases contained CO, H_2, H_2O, and CO_2.

Successful SRS measurements rely on filtering the Rayleigh line, or excitation laser, from the signal. The use of SRS for combustion diagnostics is limited by low signal levels, spatial resolution, and laser induced breakdown of particle laden flows, though despite this it has been widely employed for both laminar and turbulent gas-phase combustion studies.

2.7.3. Coherent anti-Stokes Raman scattering (CARS)

Coherent anti-Stokes Raman scattering is a variation of Raman spectroscopy where three input photons are required; a pump and Stokes photon whose frequency difference coincides with a molecule's transition of interest, and a probe photon to scatter from the oscillating polarization induced by the pump and Stokes excitation. Signal levels are orders of magnitude higher than SRS.

Stufflebeam and Eckbreth applied CARS to double-base and composite nitramine propellants [70]. They used a 10 Hz Nd:YAG laser with a pulse duration of 10 ns for measurements of temperature, CO_2, CO, N_2, H_2O, NO, H_2, HCN, and N_2O at pressures up to 35 atm. The laser probe volume was positioned 1 mm above the propellant surface at ignition and propellant allowed to burn down. They did observe incoherent emission superimposed on the resulting CARS spectra due to laser breakdown of the product gases. For future work they suggest a dual broadband CARS approach for simultaneous acquisition from three spectral regions to measure multiple species at once.

CARS spectra that were previously obtained using nanosecond pulsed lasers in a particle-laden flame, such as a metalized propellant, were determined to be severely impacted by nonresonant background as a result of the plasma formed by laser-induced breakdown of particles. Recently, Kearney [71] performed ultrafast pure-rotational CARS measurements for obtaining temperature and relative oxygen concentration in the plume of a burning, aluminized AP/HTPB propellant strand. By delaying the probe beam arrival time, background-free single-laser-shot spectra were acquired and successfully fit for temperature and relative oxygen content. The probe volume, or laser focus measurement volume, was positioned within 3 mm or less of the burning propellant surface and temperatures in excess of 3000 K were measured. Results show that ultrafast CARS is a potentially enabling technology for probing harsh, particle-laden combustion environments. However, CARS measurements requires the temporal and spatial alignment of multiple laser beams and spectral modeling which in some cases can be quite complicated. In addition, the technique is difficult to perform at elevated pressure due to collisional line narrowing. Despite its challenges, due to the direct measurement of populated states, CARS remains the most accurate experimental method for flame temperature determination.

2.7.4. Laser-induced breakdown spectroscopy (LIBS)

The technique LIBS is atomic emission spectroscopy with a high energy laser excitation source. A laser is focused onto a sample forming a plasma, enabling standoff atomic species detection. O'Neil et al. [72] performed nanosecond laser LIBS experiments to detect metal vapor concentration during composite propellant combustion. This is the first reported use of LIBS for propellant combustion diagnostics. They were able to detect aluminum at concentrations of 5, 10, 16% solids loading

within a composite propellant formulation.

3. Modeling and simulation

The extent of physical detail included in different models typically comes down to the computational efficiency. For example, two different modeling approaches are explored by separate researchers throughout the history of heterogeneous propellant combustion simulations. The first is a detailed gas-phase representation with variable thermal properties, detailed transport properties, and detailed finite-rate chemistry, but is usually steady-state in nature and does not account for the configuration of the solids loading or the surface regression. The second approach accounts for a more detailed description of the solid propellant morphology and surface regression, but lacks physical detail of the gas-phase.

One of the most cited models for the combustion of heterogeneous propellant of ammonium perchlorate and hydroxyl-terminated polybutadiene is the Beckstead-Derr-Price (BDP) model originally developed by Beckstead et al. [34] and expanded to include more features in Refs. [73,74]. The physical description of the combustion process includes the heating of the oxidizer and binder, the endothermic decomposition of both AP and HTPB, either condensed-phases or surface reactions that increase the exothermic heat release close to the solid, followed by the gas-phase reactions and transport phenomena. The BDP model theorizes three possible flames that are explicitly considered in the modeling approach; 1) the primary diffusion flame between AP and HTPB, 2) the premixed monopropellant flame occurring above the AP with an adiabatic flame temperature of 1400 K, and 3) the final diffusion flame where the products of the monopropellant flame and pyrolysis products of the binder combine in a stoichiometric ratio.

The BDP model is a one-dimensional approach that uses a uniform surface temperature and assumes the HTPB pyrolyzes in a stoichiometric ratio to the AP, with the rate of AP decomposition determined from an Arrhenius rate expression. A simplified geometrical description is used to determine the ratio of oxidizer to binder on the planar propellant surface. This approach is capable of accounting for varying particle sizes by considering the geometrical factor, h/D_o (see Fig. 4), that represents the protrusion (at low pressures) or the regression (at high pressures) of the AP in the binder matrix [75] and how this affects the propellant burning rate. This model is exercised through the adjustment of critical parameters to determine their contributions to burning rate predictions, which included the thermal conductivity (λ), heat capacity (c_p), diffusion coefficients, and condensed-phase heat release (Q_L). These values are shown to have a significant effect on the results and should be carefully considered if a model is eventually meant to be truly predictive. Factors such as the surface pyrolysis pre-exponential term (A_f), activation energy (E_f), and time to ignition had a much lesser effect on the burning rate.

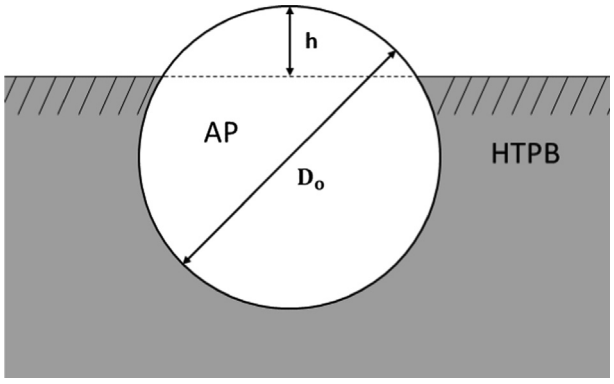

Fig. 4. Geometrical representation of a spherical AP crystal in an HTPB binder, with h representing the height of the spherical cap either protruding or regressing with respect to the planar surface of the propellant.

Heat release in the condensed-phase was studied using the BDP model by varying the liquid phase heat release (Q_L) between − 100 and − 200 cal/g, an exothermic heat release in the liquid layer of $Q_L = -120$ cal/g compared best to experimental results. It was shown that 76% of the energy release from AP occurred in the liquid layer and will have a leading order effect on the overall burn-rate. The value of Q_L was also shown to have an effect on the surface temperature, the particle size dependencies, and oxidizer concentration dependencies on the burning rate. Although this model assumes the problem to be one-dimensional in nature, steady-state, with constant properties, it highlights the importance of AP/HTPB combustion physics on predicting the characteristic burning of heterogeneous propellants. A model should include a representation of the surface geometry with varying AP particle sizes and distributions, multiple flame structures in the gas-phase including diffusion and premixed flames, detailed thermophysical properties at varying temperatures and pressures, the decomposition mechanism of oxidizer in the condensed-phase, and the coupling of the solid and gas phases at the propellant interface.

With all the complexity of solid propellant combustion, two of the most common ways to correlate models and experimental results are to compare strand burner or sandwich propellant burning rate data of different propellant formulations as described in Section 1.10. These databases have been used for quantitative and qualitative model validation, however further information of the species concentrations and temperature profiles would be immensely useful. Increased collaboration between modeling tools and experiments has the ability of highlighting important physics occurring during combustion. Recently, Maurer et al. [76] applied detailed simulations of single AP particles in HTPB coupled with a two-dimensional ray-tracing algorithm in order to understand the effects the flame temperature and species have on light sources used for optical measurements. This approach can be used to help guide future experiments and improve diagnostic capabilities that can in turn aid in the improvement of current models.

3.1. AP monopropellant

Modeling the combustion of the self-deflagration of AP is complicated in its own right without considering the polymer binder matrix used to create a complete heterogeneous propellant. Not only should the gas-phase combustion process be modeled, but the condensed-phase of AP decomposition can have a significant effect on the burning rate [77]. Guirao and Williams [18] developed one of the first models for AP monopropellant deflagration in 1D accounting for the exothermic heat release in the condensed-phase and including a detailed, 14-step reaction kinetics in the gas-phase. This model was used to compare to experimental burn-rates of AP monopropellant from 20 to 200 atm. The AP (NH_4ClO_4) can either go through dissociative sublimation to create ammonia (NH_3) and perchloric acid ($HClO_4$) or can undergo decomposition through condensed-phase reactions with the deflagration products consisting of primarily: H_2O, O_2, HCl, N_2, NO, Cl_2, and N_2O in stoichiometric proportions. The model showed good overall agreement up to 100 atm, but does not capture the decrease in burn-rates at higher pressures observed through experimentation. Both the gas and condensed-phase reactions play a critical role in determining the heat release to the surface and thereby controlling the burn-rate, however this model had a fixed value to define the ratio of condensed-phase and gas-phase reactions which could be invalid at higher pressures. Different physics at the surface are needed to better describe the decomposition and could include gas absorption at the liquid layer or a disappearance of the liquid layer entirely.

Manelis and Strunin [78,79] developed a model to simulate the combustion of AP through an exothermic description of the condensed-phase reactions coupled with the sublimation. It was theorized that two processes compete to get different burning rates versus pressure, the increase in surface temperature and the decrease of perchloric acid with increasing pressure. To model the burning rate accurately, emphasis

was placed on the condensed-phase decomposition of AP. Common assumptions made in the modeling approaches are to assume constant specific heats in all phases, constant thermal conductivities, constant species diffusivities, and an estimate of the premixed flame standoff distance. Price et al. [80,81] developed a model (Price-Boggs-Derr model) that used the finite-differencing method and tabular thermal properties in order to eliminate these assumptions. In this model, a linear c_p model is used for each phase, thermal conductivity is tabulated, and tabulated heats of formation and flame temperatures are used. Attention is given to the phase transition in the solid phase, the condensed-phase reactions, and to a more detailed gas-phase representation with variable thermal properties. The Price-Boggs-Derr model was expanded upon by Shusser et al. [82] to investigate the unsteady response of AP combustion by adjusting the kinetic parameters to better match experimental burn-rates and compared to an exact analytical solution for a linear response. Results showed the applied pressure wave form had a direct effect on the combustion response even with similar amplitude and frequencies and is capable of extinguishing the AP flame during deflagration.

Miller and Coffee [83–85] used a similar approach to Price, but instead utilized the Finite Element (FE) method to discretize the numerical solution. It is a 1D, steady-state model that uses a linear burn-rate model at the surface and assumes constant c_p and λ in the gas-phase, unity *Le* number, a single pyrolysis model, and a global 1-step reaction mechanism to model heat release. This model was compared to the "classical approach" of semi-analytical solutions and experimental data. It showed the temperature sensitivity, σ_p, was very sensitive to the combustion model chosen. It emphasized the need to compare to the physics based detail of experiments rather than solely looking at burning rates which would require a better understanding of the solid and condensed-phases through the use of embedded thermocouples [86] and a better understanding of the condensed-phase kinetics.

Further model development includes the unsteady solution to investigate combustion stability of AP and the addition of detailed chemical kinetics and transport data in the gas-phase. Sahu et al. [87] introduced a new reaction mechanism with 22 reactions and 18 species that extends upon the work of Guirao and Williams [18]. This model assumes 70% of the AP reacts in the condensed-phase to be consistent with previous models and reduces the amount of ammonia present in the gas-phase. Ramakrishna et al. [88] used a 1D, unsteady combustion model to explore the stability response of AP deflagration, specifically looking at the major factor in the low pressure deflagration limit (LPDL) of AP. A non-constant value of the condensed layer is assumed for the first time to be a linear function of temperature with a value of the condensed-phase undergoing exothermic decomposition represented in a fractional form as, f; $f = 0$ below the melt temperature of AP ($T_s < 825$K), it increases with T linearly as, $f = 0.6 - 0.024(850 - T_s)$, until the maximum value of $f = 0.6$ is used for any temperature above $T_s > 850$ K. Surface heat release is also a function of f, ranging from -205 kJ/kg $< Q_L < 1.85$ MJ/kg, from $f = 0.6$ to $f = 0$, respectively. A 1D, unsteady model with a single-step gas-phase reaction, surface pyrolysis law, with unity Le and Prandtl (Pr) numbers is used to solve the conservation of mass, species, momentum, and energy equations. The model is validated against experimental data and then used to exercise fundamental values to better understand their importance on the combustion process. Higher values of the activation energies for the pyrolysis law and the gas-phase (single-step) reaction have seen success in steady-state models, but prove to be unstable in an unsteady solution. The LPDL limit was observed to be caused by a loss of the melt layer and a transition to an endothermic reaction at the surface resulting in a flame out. By solely including a heat loss mechanism at constant f, then flame out will only occur if heat losses are greater than the heat provided by the condensed-phase reactions and therefore, the proper mechanism for the LPDL limit should be the modeled as the loss of the melt layer.

Detailed gas-phase kinetics are further developed by Giovangigli et al. [89] including 37 species and 215 reactions. A one-dimensional model is developed with the coupling of the liquid and solid phases being accomplished through the use of continuation techniques due to the ad-hoc nature of the condensed-phase kinetics resulting from the lack of available experimental data in this regime. The surface is treated as a dual-reaction in which the AP can sublimate or decompose at a constant temperature instead of modeling it as a melt layer and found that 40% of the AP decomposes at both low and high pressures. This model attributes the extinguishment at the LPDL as a function of heat loss as opposed to the lack of a melt layer. Rahman et al. [90] expanded on this model to include variable properties in the solid-phase and relaxed the constant surface temperature assumption by using a pyrolysis law. The unsteady combustion of AP was studied observing the importance of the pyrolysis activation energy on the stability of the solution with higher values leading to an unstable result. Due to the inherent instabilities of the AP combustion at high pressures and lower initial temperatures, a quasi-steady approach is only appropriate for low pressures and low oscillation frequencies due to chemical, convective, and thermal propagation time scales.

More recently, Vo et al. [91] introduced a mathematically rigorous model that accounts for the solid, liquid, and gas phases in terms of coordinate transformations in each phase that range from 0 to 1 in the solution domain. The energy release from solid to liquid AP is considered, a detailed condensed-phase reaction scheme is taken from Jeppson et al. [92] and a reduced reaction set is applied to the gas-phase. The solution is progressed in 1D cylindrical coordinates with two moving boundaries at the solid-liquid and liquid-gas interface to estimate the burning rate, temperature profile, species distribution, and phase thicknesses. Good overall agreement to the burning rate data was observed with values predicted by the simulation comparing to experimental results within 10%. McQuaid and Chen [21,22] have been developing a finite-rate mechanism for gas-phase reaction kinetics of AP species using high-level quantum mechanics based electronic structure methods, and applying statistical mechanics and transitional state theories to create a reaction scheme with 788 reactions and 105 species with particular focus on the chlorine oxides and acids. This mechanism was reduced to 44 species and 84 reactions and applied in a 1D model to exercise the reaction scheme and explore the steady-state combustion of AP monopropellant deflagration with coupling of the solid and gas phases. Experimentally, a liquid layer with bubbles is observed for AP combustion in the pressure ranges of 20.4–54.4 atm, from 54.4 to 68.0 atm the observed liquid layer transitions from a froth to a pattern of ridges and valleys at 68.0–136 atm, from 136 to 272 atm unsteady combustion is observed with needle-like formations on the surface, above 272 atm other surface physics will need to be considered to capture the burning rate. None of these features are modeled in this study, allowing for the effects of finite-rate chemistry on the AP burning rate to be assessed independently. Different pyrolysis laws were used to model the surface regression with little observable effect on the overall burning rate. The model was able to capture the burning rate behavior in the range of pressures between 20.4 and 136 atm, but continued to predict a linear burn-rate at pressures above 136 atm, although the experimental data exhibits a sharp decrease due to combustion instabilities. The results provide strong evidence that the newly developed kinetics are applicable at lower pressures and the slope break in the data with increasing pressure is most likely due to a surface or condensed-phase phenomena that require additional consideration rather than solely relying on the gas-phase chemistry. Although, the ultimate goal is to model a heterogeneous propellant, more knowledge is required for the condensed-phase chemistry, the concentration and evolution of gaseous species of AP and various binders, and the detailed reaction chemistry occurring in all phases.

3.2. Gas-phase modeling

The gas-phase representation of heterogeneous propellant

combustion has taken on many forms throughout history, from a non-dimensional representation to simplified approaches with constant properties to solving the complete Navier-Stokes equations with a detailed description of the transport and chemical kinetic processes. Considering the gas-phase portion of the model is only a part of the overall solution, no one model is necessarily better than any other. However, it is important to understand the assumptions made during the mathematical formulation in order to better understand their implications on the final results and the solution regimes these assumptions tend to break down.

The earliest combustion models relied on empirical fits to model the linear burning rate seen in experiments and included a set of analytical equations for relatively efficient computations [34,40,93,94]. Miller et al. [40] used an empirically based model and extended the granular diffusion flame (GDF) model of Summerfield [95] to investigate the burning rate of polydisperse AP propellants modeled with a linear burn-rate model and demonstrated an upper and lower limit on the burn-rate with respect to pressure. Merzhanov et al. [93] used powdered AP and binder to simulate a heterogeneous propellant within a TGA/DSC and used the regression data to fit burn-rate kinetics.

Eventually, analytical methods lost favor to discretized approaches using the finite difference [80], finite element [83], and finite volume methods [38], which were capable of extending the solution to multiple dimensions beyond a zero or first order approach. Discretization is currently the preferred numerical approach for modeling and simulation in order to eliminate assumptions needed to close a set of equations in an analytical approach. However, the equations being discretized have their own set of assumptions in order to simplify the problem and reduce computational demand. Buckmaster et al. [96] developed a non-dimensional, 2D gas-phase model with the transport equations written in terms of the Peclet number (*Pe*) and the Lewis number (*Le*) to define the ratio of advective to diffusive transport and the ratio of thermal to mass diffusivities, respectively. The reaction rates are written in terms of the Damköhler (*Da*) number and is used to represent the ratio of kinetic to diffusion transport rates. Two reactions are considered in the gas-phase that represent the AP deflagration and the heat release of combining AP and HTPB. The *Pe* and *Da* number were adjusted to observe changes in flame shape and burn-rate, e.g. extinguishment at low *Pe* and *Da* can occur corresponding to sudden pressure drops. Chorpening et al. [54] extended this model and used it to observe the burning behavior of a sandwich AP/HTPB propellant and compared to experimental results. By adjusting the *Pe* and *Da* parameters, a general understanding of the combustion physics can be obtained. Low *Pe* and *Da* correspond to low pressure and low convection scenarios, which give a broad reaction zone of the sandwich propellant connected over the fuel. Increasing the *Pe* and *Da* numbers result in a primary flame between the fuel and oxidizer with localized heat release at the surface closest to the flame. Jackson and Buckmaster [97] used a similar model to explore the effects of a changing *Le* number to simulate the effects of unsteady combustion on the 2D flame. When *Le* is high enough to simulate large heat losses, oscillating instabilities that are characteristic of premixed flames are observed.

To increase fidelity of the gas-phase modeling of AP/HTPB propellant combustion the development of finite-rate kinetics is studied and utilized in discretized models. Ermolin et al. [98,99] investigated the combustion of AP and AP based propellants experimentally and numerically to determine reaction mechanisms. This work focused on capturing the kinetic processes of AP combustion consisting of, 1) the reversible dissociative sublimation of AP with the formation of NH_3 and $HClO_4$, 2) irreversible AP decomposition reaction occurring in the condensed-phase parallel to the sublimation process, and 3) gas-phase decomposition of $HClO_4$ and the oxidation of NH_3 in the premixed flame zone. These studies used low pressure flames ($\sim$0.1 atm) and mass spectroscopy to determine species compositions. An initial mechanism of this process was created for the elements of N, H, Cl, and O containing 24 species and 80 reactions, with NO and N_2O revealing themselves as major components of nitrogen which would otherwise be unobservable solely using chemical equilibrium calculations. Korobeinichev et al. [51,52] extended the previous work by including a polybutadiene rubber component, introducing the carbon atom to the list of elements. A kinetic mechanism for this system consisted of 49 species and 243 reversible reactions. A sensitivity analysis of an AP/butadiene planar flame showed the reactions, $NH_2 + O_2 = HNO + OH$ and $ClO + CO = Cl + CO_2$, had the greatest effect on the combustion zone width. Ermolin et al. [100 101] specifically explored the $NH_2 + O_2 = HNO + OH$ reaction in order to solidify the rate constant and make it relevant for higher pressures that would occur in realistic combustion environments. Further improvement and mechanism reduction was conducted by Ermolin et al. [102] to better estimate the rates of perchloric acid-ammonia flames. This work along with the development of the hydro-carbon kinetic mechanism from the Gas Research Institute (GRI-Mech) [103] has enabled modelers to include detailed finite-rate chemistry in the gas-phase combustion solvers.

Smooke et al. [66,104] utilized the kinetic mechanisms described above in a steady-state, 2D velocity-vorticity finite-difference formulation to investigate a methane/AP co-flow flame and a counter-flow diffusion flame of ethylene and AP. The model includes detailed transport properties and finite-rate chemistry consisting of 86 species and 506 reactions, to determine the velocity, vorticity, species composition, and temperatures in the flame zone. Experimental results were used to set the mass flow rate of gases at the boundaries and the regression rate of the AP crystals. A better understanding of the reaction zones and combustion processes of heterogeneous propellants can be explored with this model. Improvements would include the condensed-phase reactions and a gaseous mixture of acetylene and ethylene to better represent the products of HTPB pyrolysis. Gross and Beckstead [105,38,106] also utilized the combined mechanisms of Ermolin and GRI to conduct steady-state, 2D velocity-vorticity calculations using a finite-volume approach. This model considers a single AP particle surrounded by a homogenized binder with the equations represented in 2D cylindrical coordinates. The surface is assumed to be planar with no heat conduction occurring into the solid, the AP and homogenized binder pyrolize according to an Arrhenius rate. Using the detailed gas-phase approach, the changes in flame shape, surface heat flux, and local burn-rate are investigated as a function of AP particle size and ambient pressure. At low pressures and small particle sizes, the premixed limit of the propellant is reached and a distinct flat flame over the propellant is observed as opposed to the primary flame attaching at the AP/HTPB interface. The burn-rate can be seen to plateau at the premixed limit for low pressures and small particles, and also at the AP deflagration limit at high pressures and large particle sizes. More recently, Nusca [107,108] has developed an unsteady, explicit 2D solver with finite-rate chemistry to model the combustion of sandwich propellants with surface regression. This model uses a new skeletal kinetic mechanism under development at the Army Research Laboratory [109] reduced from the larger AP/HTPB mechanism of Ref. [110] and compares to experimental burn-rates of sandwich propellant with a good degree of accuracy. A new surface crack and de-wetting model for the high pressure regime is considered and observed to capture the experimental burn-rate increase.

Applying the increased level of detail in the gas-phase is generally computationally expensive and limits the solution domain to the micron-scale, while a simplification of the equations in terms of non-dimensional numbers, i.e. *Pe*, *Le*, *Pr*, *Da*, etc., and/or reducing the kinetic scheme to fewer than five steps can allow for more detailed descriptions of the propellant on larger scales and in multiple dimensions. The sandwich propellant has been a useful configuration for modeling [111,96,112,113,114] in that it reduces to an essentially 2D problem and eliminates the need to resolve micron sized AP in the propellant matrix. Hegab et al. [115,116] developed a 2D model with an Oseen approximation and a global kinetic mechanism to solve the combustion of a sandwich propellant. Burning rate was determined from a surface

tracking algorithm developed via a single-value coordinate transformation, with the surface coordinate moving at the speed of the local regression defined by the pyrolysis rate laws of AP and HTPB. Burn-rate versus pressure was compared to experimental data. Ramakrishna et al. [117,114] introduced a similar model with a 3-step kinetic scheme to represent the AP decomposition flame, the primary flame (leading edge flame), and the final diffusion flame. The full Navier-Stokes equations are considered and the 2D heat conduction into the solid is modeled along with the surface regression. Both modeling approaches consider *Pr* and *Le* to be constant which can restrict the influence of diffusional effects by not accounting for differential diffusion and heat transfer. Gross et al. [118] used the micro-scale, 2D velocity-vorticity formulation with finite-rate chemistry to reduce the flame description to four distinct flame shapes; 1) premixed AP monopropellant flame, 2) the primary flame between oxidizer and binder, 3) the final diffusion flame, and 4) the premixed homogenized binder flame, into a set of 4-step reaction kinetics that can be used in a meso-scale model. Comparisons to different experimental propellant burning rates were shown to be within ± 10%. Gaduparthi et al. [119] used a simplified approach with constant *Pr* and *Le*, a mid-level approach with detailed transport and a reduced order mechanism, and a detailed transport and kinetic model to simulate the combustion of a sandwich propellant described experimentally by Navaneethan et al. [120]. The detailed kinetics proved to be too computationally expensive to be a viable option, while the mid-level approach showed much greater detail in the flame shape and emphasized the importance of including detailed thermal and transport properties.

3.3. Solid-phase modeling

The importance of the solid phase modeling, especially the AP size distribution, heat transfer, and condensed-phase reactions have been acknowledged in the earliest models. Different levels of approximation have been used, with the overall objective of completely representing a three-dimensional, real world propellant to high degree of accuracy and computational efficiency. The first attempt to model a three-dimensional propellant with distributed flame structure and surface heat flux was developed by Jackson et al. [121], with the AP distribution modeled as a periodic array. To advance this approach, Knott et al. [122] developed a random packing algorithm that idealizes the AP crystals as either disks (2D) or spheres (3D). This model was validated against steel-shot data to ensure the randomly assorted spheres could match the theoretical pack densities. Fig. 5 shows a representation of the AP particles idealized as disks (a) and as spheres (b) for a tri-modal distribution of AP crystals in an HTPB binder. A three-dimensional representation of the solid propellant is critical to fully understand the combustion of heterogeneous propellant as the AP size distribution can have a significant effect on the burning rate, pressure exponent, and other propellant characteristics. Jackson and Buckmaster [123] used the above packing algorithm to define a randomly packed, 2D solid propellant that could be modeled in their combustion solver. A level-set is used to distinguish between the AP and binder and a homogenization theory is used to determine the thermal properties in the solid-phase. The model was used to explore the oscillating effects of propellants with varying *Le* number and observations of the local equivalence ratio were tracked with the regressing surface. Massa et al. [124] extended the randomly packed propellant algorithm to explore the combustion of 3D propellants with a 3-step kinetic mechanism. Rajoriya et al. [125] used a randomly packed algorithm to investigate the thermal diffusivity and thermal conductivity numerically and compared their results to available experimental data. Caution must be taken when considering homogenization of solids in the polymer matrix, especially when the thermal conductivities of the constituents vary largely.

The common assumption for AP shapes are either disks in 2D or spheres in 3D, but in actuality the AP could be highly irregular as seen in Fig. 1. Wang et al. [126] attempted to quantify the effects of AP shape on the burning rate considering the AP to be ellipses/ellipsoids in 2D/3D, respectively. With the ellipses oriented in the same direction, the burn-rate can be altered by ~ 50%. However, if the directionality of the elliptical AP particles is also randomized, the burn-rate was altered between 4 and 8% with larger variations being observed at the higher pressures. Plaud et al. [127] also studied the effects of particle shape and orientation using a 3D combustion model for AP/HTPB solid propellant burning. The study found the orientation of the ellipsoids had a significant effect on the burning rate and could be a contributing source of uncertainty when trying to model the randomly oriented, unevenly distributed AP particles of a real-world propellant.

Aside from the solid propellant distributions, it is also important to include the condensed-phase reactions, melt layers, etc. that are important in modeling the single component AP during self-deflagration. Murphy and Krier [128] studied the use of two surface models, one with a single condensed layer and the other representing a double-reaction molten binder layer covering the propellant surface. The latter showed better agreement comparing against the frequency response of experimental data and supports the assumption of a liquid binder layer on the surface that shields AP from direct heat transfer from gas-phase flames. In an attempt to include a detailed condensed-phase reaction mechanism, Jeppson et al. [92] used a 1D model to represent the solid, liquid, and gas phases with phase transition in the solid, condensed-phase reactions, and a detailed gas-phase description including the finite-rate chemistry of Korobeinichev et al. [52] and the GRI-Mechanism [103]. The condensed-phase reactions were shown to have a leading order effect on the propellant burn-rate; however, it is difficult to validate these reaction steps without corresponding experimental data. In fact, Gusachenko and Zarko [129] argue for the need of condensed-phase reactions in a propellant model due to the large effects on surface heat flux and burn-rate. To this point researchers have relied on gas-phase reactions to dictate the controlling factors of the combustion process, but models could be improved with the use of accurate condensed-phase reactions, heterogeneous reactions at the surface, the inclusion of a melt layer, and the possibility of heat from the burning surface being conducted to the subsurface reaction zone to better capture burn-rates.

3.4. Interface tracking and phase coupling

With models of the solid, liquid, and gas phases in place, one of the remaining issues to address is the interface jump conditions between phases and the methods to track the surface regression. Hegab et al. [115] use one of the most common forms of coupling and surface regression, deploying pyrolysis laws for the AP and HTPB to describe the localized regression rate, assuming thermal equilibrium between the gas and solid interface, and tracking the surface using a coordinate transformation. The surface coordinate is expressed as, $\eta(x, y, z, t) = 0$, where the surface is assumed to only move in the y-coordinate, such that $\eta = y - f(x, z, t)$ and a Hamilton-Jacobi equation is solved to track the surface. This assumption is good as long as the surface does not decrease sharply in a region to become parallel with the y-axis. To allow for irregular surfaces and possibly spalling or energetic particles releasing from the surface, one can consider the approach of Wang et al. [130,131], Cazan and Menon [132], and Choi et al. [133] where a level-set function is applied to the interface and the surface motion is tracked solving the distance-sign function coupled with the surface regression rate as a function of time. This leads to challenges in the numerical approach as the surface intersects computational grid cells, but can be overcome using a cut-cell approach [132,133]. Further advancements to the interface modeling would be the inclusion of detailed condensed-phase reactions and heterogeneous surface reactions to eliminate the need for pyrolysis rate laws to describe the regression of AP and HTPB from empirical data fits.

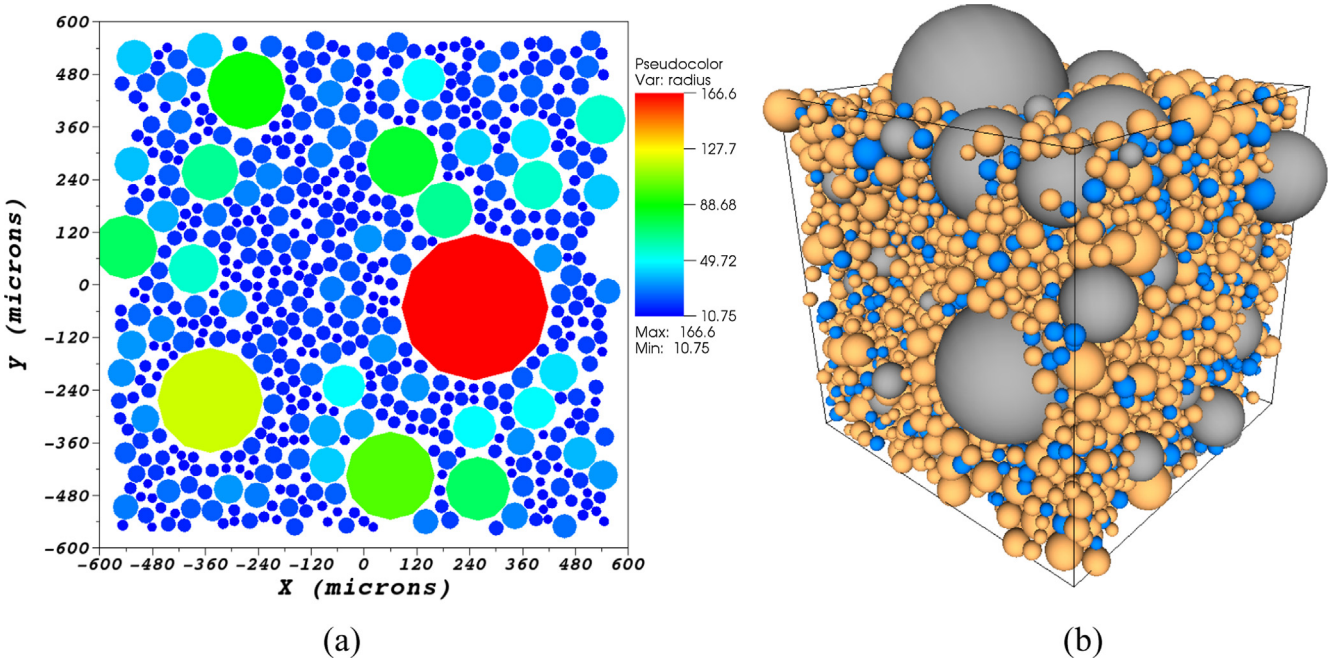

Fig. 5. Representations of a tri-modal distribution of AP crystals within a binder idealized as (a) cylinders in 2D and (b) spheres in 3D. The 2D scale shows the varying radii of the AP and the 3D sphere colors represent a statistical particle size distribution ranging in size from the smallest (blue) to the largest (silver). (For interpretation of the references to colour in this figure legend, the reader is referred to the web version of this article.)

3.5. Applications of current models

A truly useful model is one that can provide valuable insight into a problem that could otherwise not be done experimentally or can be achieved in a safer or more cost-effective manner. For instance, there is limited data on the unsteady combustion effects and erosive burning of solid propellant, but modeling can help provide understanding to these scenarios. Surzhikov and Krier [134] developed an unsteady dynamic variables (UDV) method for solving the unsteady Navier-Stokes equations while still maintaining an efficiency equivalent to the vortex-stream function formulation. This model was used to investigate the transient combustion of an alternating AP/HTPB propellant with varying flame structures for differing gravitational fields. Favale and Miccio [135] used an unsteady model to explore the response of propellant burning with an applied periodic pulsating heat flux, where the propellant will burn at the same frequency when a low frequency perturbation is applied. Buckmaster and Jackson [136] and Topalian et al. [137] investigated the effects of shear on the burn-rate and observed the largest effect occurred on the primary diffusion flame, such that a decrease in the AP diameter would decrease the effect of shear and less erosive burning is observed as the premixed limit is approached. Massa et al. [138], Cai et al. [139], McDonald and Menon [140] and Isfahani et al. [141] separately investigated the erosive burning of a solid propellant coupled with the cross-flow of a rocket motor, which is the eventual application of a solid propellant combustion model. Unsteady models have also been applied to increase the understanding of depressurization effects on burning propellant [142] or the ignition process at different applied heat fluxes [143]. Modeling is also used to explain the burn-rate effects of a propellant including aluminum particles [130,144,145] which can include the complication of aluminum agglomeration, particle tracking, aluminum burning, a particle release model, and radiation heat transfer to the surface.

4. Conclusions

The combustion of ammonium perchlorate (AP) and hydroxyl-terminated polybutadiene (HTPB) solid composite propellant is a complex, multiphase process that includes condensed-phase kinetics, heat and mass transfer, premixed and diffusion flames, and complex burning geometries. Extreme temperature and density gradients in the gas-phase create a challenging environment to diagnostically probe and requires a computational domain to be small enough to accurately represent heat fluxes and transport processes. Solid and liquid phases are difficult to probe with non-intrusive techniques and simulations rely on simple models to describe the thermal decomposition with limited empirical data for validation. The most recent reviews on the topic of propellant combustion have also been provided by Beckstead et al. [146] and a modeling review of heterogeneous propellant has been given by Jackson [147].

To continue to develop, validate, reduce, and refine computational models additional experimental data is required. Experiments are challenging; solid composite propellant flames are extremely luminous with dense products and smoke, causing difficulty seeing through the flame. Steep density and temperature gradients, and thin reaction zones which vary as a function of time require measurement techniques with high dynamic range, spatial, and temporal resolution. Furthermore, propellants are designed to operate at elevated pressure, experimental validation is needed for representative rocket motor pressures of at least ~47.6–68.0 atm. Diagnostics need to be developed and applied for measurements at elevated pressure and for polyatomic species not previously investigated but believed to play an important role, such as NH_2, HNO, and ClO_2.

The greatest lack of experimental work is in the investigation of condensed-phase processes. Experiments that have been performed to understand the condensed-phase were typically performed at low pressures, under laser-assisted conditions, and measured a single global reaction rate. The condensed-phase is difficult to study due to phase heterogeneity, spatially small reaction zones, steep temperature and concentration gradients, and the formation of carbonaceous residue. Measurements of species concentrations, thermal profiles, solubility and kinetic parameters, particle-binder interaction energy, and binder cross link density are needed.

In general, experimental techniques are advancing and are starting to be available at the time and length scales relevant to solid propellant

combustion. This is due to advances in sensor and laser technology and diagnostics development for fundamental and applied turbulent combustion research. Such diagnostics are just recently being applied to solid propellants, for example tunable diode laser absorption spectroscopy (TDLAS) was used for measurements in the plume of a gas generator [148]. As more data becomes available, care should be made when comparing M&S results to experimental data regarding initial and boundary conditions.

The ideal computational model for AP/HTPB combustion would be predictive in terms of the flame characteristics and surface regression as a function of AP size distribution, initial temperature, and ambient pressure. Gas-phase thermal and transport properties have been shown to play a critical role on the burning rate and assumptions of constant properties should be relaxed, especially near the surface, to better capture the flame characteristics and heat feedback. Finite-rate chemistry in the gas-phase is important, but cannot be the only factor included when attempting to capture the slope breaks in burning rates of AP composite propellants. Condensed-phase reactions have a significant effect on the overall burn-rate and require a more accurate kinetic mechanism, eliminating the need for empirical pyrolysis laws to describe AP and HTPB decomposition. Also, a better understanding of the decomposition of HTPB is critical. There is uncertainty associated with HTPB depending on the molecular weight, cross-linking, etc. that would require research to tabulate thermal and transport properties, and heat of formation as a function of varying HTPB binders [92]. Modeling the complex combustion instabilities of pure AP requires a detailed condensed-phase model with either a transitioning liquid layer or a model for the varying surface area due to cracks/spalling. The particle size and distribution of AP are two factors that dictates the unique burn-rate of a specific propellant formulation; an accurate simulation of these effects requires a multi-dimensional model with surface regression and detailed interface coupling between phases. A singled-valued surface coordinate transformation has been shown to be successful in tracking the moving interface, but is limited to semi-planar surfaces. Complex geometries can be captured using a level-set surface tracking algorithm, however these methods require creative mathematical formulations to ensure the surface heat flux is appropriately accounted for; which could include the use of automated mesh refinement (AMR). An unsteady formulation is ideal for capturing combustion instabilities of a rocket propellant and would require the model to capture time-scales associated with convection, combustion, and acoustic wave propagation. A complete description of propellant combustion would include all of these aspects and be computationally efficient using a highly parallelized system.

Acknowledgments

This work was sponsored by the Air Force Research Lab, Office of Naval Research Advanced Energetic Materials Program, and the NAVAIR In-House Laboratory Independent Research Program managed by ONR.

References

[1] Edwards TJ. Solid propellant flame spectroscopy. CA: Edwards Air Force Base; 1988.
[2] Isert S, Hedman T, Lucht RP, Son SF. Oxidizer coarse-to-fine ratio effect on microscale flame structure in a bimodal composite propellant. Combust Flame 2016;163:406–13.
[3] Steinz JA, Stang PL, Summerfield M. The burning mechanism of ammonium perchlorate based composite solid propellants. Princeton, NJ, 1969.
[4] Zanotti C, Volpi A, Bianchessi M, De Luca L. Measuring thermodynamic properties of burning propellants. Nonsteady burning and combustion stability of solid propellants. American Institute of Aeronautics and Astronautics, Inc.; 1992. p. 145–96.
[5] Kubota N, Kuwahara T, Miyazaki S. Combustion wave structures of ammonium perchlorate composite propellants. AIAA 20th joint propulsion conference. Cincinnati, OH; 1984.
[6] Alspach DA. Temperature measurements through a solid-propellant combustion wave using embedded fine wire thermocouples. Air Force Astronautics Laboratory; 1990.
[7] Sabadell AJ, Wenograd J, Summerfield M. Measurement of temperature profiles through solid propellant flames using fine thermocouples. AIAA J 1965;3(9):1580–4.
[8] Vanderhoff JA, McQuaid M, On propellant surface temperatures derived from calorimetry, Aberdeen Proving Ground, 2001.
[9] Zenin AA. Thermophysics of stable combustion waves of solid propellants. Nonsteady burning and combustion stability of solid propellants. American Institute of Aeronautics and Astronautics, Inc.; 1992. p. 197–231.
[10] Lengelle G, Duterque J, Trubert JF. Physico-chemical mechanisms of solid propellant combustion. Solid Propellant Chemistry, Combustion, and Motor Interior Ballistics. American Institute of Aeronautics and Astronautics, Inc.; 1999. p. 287–334.
[11] Beckstead MW, Hightower JD. On the surface temperature of deflagrating ammonium perchlorate crystals. AIAA 5th Aerospace Sciences Meeting. 1967.
[12] Keenan AG, Siegmund RF. The thermal decomposition of ammonium perchlorate – a literature review, Special Report No. 6, 1968.
[13] Brill TB. Combustion characteristics of crystalline solid oxidizers and lattice dynamics in ammonium perchlorate, Air Force Office of Scientific Research No 1976 AFOSR-TR-76-1176.
[14] Kalman J, Hedman T, Varghese B, Dagliyan G. Nano-computed tomographic measurements of partially decomposed ammonium perchlorate particles. Propellants Explos Pyrotech 2017;42(9):1111–6.
[15] Herley JP, Levy PW. Radiation-induced Dislocations in Ammonium Perchlorate Crystals. Nature Phys Sci 1971;232:66–8.
[16] Majda D, Korobov A, Filek U, Sulikowski B, Midgley P, Nicol D, et al. Low-temperature thermal decomposition of crystalline partly and completely deuterated ammonium perchlorate. Chem Phys Lett 2011;504(4):185–8.
[17] Boggs TL, Price EW, Zurn DE. The deflagration of pure and isomorphously doped ammonium perchlorate. Symp (Int) Combust 1971;13(1):995–1008.
[18] Guirao C, Williams F. A model for ammonium perchlorate deflagration between 20 and 100 atm. AIAA J 1971;9(7):1345–56.
[19] Zarko VE, Gusachenko LK. Simulation of Energetic Materials Combustion, Saint Petersburg, RUS, 2000.
[20] Vyazovkin S, Wight CA. Kinetics of thermal decomposition of cubic ammonium perchlorate. Chem Mater 1999;11:3386–93.
[21] Chen C-C, McQuaid MJ. Modeling the deflagration of ammonium perchlorate at pressures from 300 to 30,000 psia. Part I: gas-phase, finite-rate, chemical kinetics mechanism development, in JANNAF Combustion Meeting 2014 Albuquerque.
[22] McQuaid M, Chen C-C. Modeling the Deflagration of Ammonium Perchlorate Pressures from 300 to 30000 PSIA. Part II: Considerations besides the Gas-Phase, Finite-Rate Chemical Kinetics Mechanism, in JANNAF Combustion Meeting 2014 Albuquerque.
[23] Boggs TL. Deflagration rate, surface structure and subsurface profile of self-deflagrating single crystals of ammonium perchlorate. AIAA J 1970;8(5):867–73.
[24] Hightower JD, Price EW. Combustion of ammonium perchlorate. Symp (Int) Combust 1967;11(1):463–70.
[25] Chen C-C, MdQuaid M. Thermochemical and kinetic studies of the pyrolysis of hydroxyl-terminated polybutadiene. In: JANNAF Combustion Meeting, La Jolla, 2009.
[26] Chen C-C, McQuaid M. Thermochemistry and kinetics modeling of hydroxyl-terminated polybutadiene-red fuming nitric acid (HTPB-RFNA) systems. In: JANNAF combustion meeting, Colorado Springs, 2010.
[27] R. Miller, H. L. Stacer and B. Goshgarian, “Effects of curative type on the ballistics of reduced smoke htpb propellant,” in 19th JANNAF Combustion Meeting, Greenbelt, 1982.
[28] Chen J, Brill T. Chemistry and kinetics of hydroxyl-terminated polybutadiene (HTPB) and diisocyanate-HTPB polymers during slow decomposition and combustion-like conditions. Combust Flame 1991;87:217–32.
[29] Cohen NS, Fleming RV, Dew R. Role of binders in solid propellant combustion. AIAA J 1974;12(2):212–8.
[30] Rao RM, Radhakrishnan TS. Thermal decomposition of polybutadienes by pyrolysis gas chromatography. J Polymer Sci 1981;19(12):3197–208.
[31] Didikin BP, Korobeinichev OP, Orlov VN. Kinetics and mechanism of the thermooxidative destruction of polybutadiene rubber in perchloric acid vapor. Combustion, Explosion, and Shockwaves 1983;19(3):239–334.
[32] Boggs TL, Kraeutle KJ. Decomposition and Deflagration of Ammonium Perchlorate, China Lake, CA, 1968.
[33] Atwood AI, Boggs TL, Curran PO, Parr TP, Hanson-Parr DM, Price CF, et al. Burning rate of solid propellant ingredients, Part 1: Pressure and initial temperature effects. J Propul Power 1999;15(6):740–7.
[34] Beckstead M, Derr R, Price C. A model of composite solid-propellant combustion based on multiple flames. AIAA J 1970;8(4):2200–7.
[35] Strunin VA, Manelis GB. Analysis of elementary models for the steady-state combustion of solid propellants. J Propulsion Power 1995;11(4).
[36] Strunin VA, Nikolaeva LI. Influence of additives on the characteristics of the combustion of layered systems imitating composite propellants. Combustion, Explosion, and Shockwaves 2017;11(3):419–28.
[37] Derr RL, Boggs TL. Role of SEM in the study of solid propellant combustion: Part III. The surface structure and profile characteristics of burning composite solid propellants. Combust Sci Technol 1970;1(5):369–84.
[38] Gross M, Beckstead M. Diffusion flame calculations for composite propellants predicting particle-size effects. Combust Flame 2010;157:864–73.
[39] Foster RL, Miller RR. The influence of the fine AP/binder matrix on composite propellant ballistic properties. In: 17th JANNAF combustion meeting, 1980.

[40] Miller R, Hartman K, Myers R. Prediction of ammonium perchlorate particle size effect on composite propellant burning rate. In: JANNAF solid propulsion meeting, Washington DC, 1970.
[41] Fry RS, DeLuca L, Freferick R, Gadiot G, Strecker R, Besser H-L, Whitehouse A, Traineau J-C, Ribereau D, Reynaud J-P. Evaluation of methods for solid propellant burning rate measurement. In: RTO AVT Specialists' Meeting "Advances in Rocket Performance Life and Disposal", Aalborg, Denmark, 2002.
[42] MIL-STD-286C, Military standard: propellants, solid: sampling, examination and testing, 1991.
[43] Miller R, Donohue M. Control of Solids Distribution in HTPB Propellants. In: JANNAF combustion meeting, Monterey, 1976.
[44] Miller R, Donohue M, Martin J. Control of Solids Distribution I – Ballistics of non-aluminized HTPB propellants. In: JANNAF combustion meeting, Monterey, 1976.
[45] Miller R, Donohue M, Peterson J. Ammonium perchlorate size effects on burn rate – possible modification by binder type. In: JANNAF combustion meeting, Monterey, 1976.
[46] Foster R, M. R.R., The burn rate temperature sensitivity of aluminized and non-aluminized HTPB propellants, In: JANNAF propulsion meeting, Monterey, 1980.
[47] Price E, Sigman R, Handley J. Microstructure of the combustion zone of composite solid propellants. In: JANNAF Combustion Meeting, Newport, 1979.
[48] Price E, Panyam R, Sambamurthi J, Sigman R. Combustion of ammonium perchlorate-polymer sandwiches. In: JANNAF combustion meeting, Greenbelt, 1982.
[49] Lee S-T, Price E, Sigman R. Effect of multidimensional flamelets in composite propellant combustion. J Propul Power 1994;10(6):761–8.
[50] Korobeinichev OP. Dynamic flame probe mass spectrometry and condensed-system decomposition. Combustion, Explosion, and Shockwaves 1987;23(5):565–76.
[51] Korobeinichev OP, Chernov AA, Emel'yanov ID, Ermolin NE, Trofimycheva TV. Investigation of the kinetics and the chemical reaction mechanism in the flame of a mixed compound, based on ammonium perchlorate and polybutadiene rubber. Combustion, Explosion, and Shockwaves 1990;26(3):292–300.
[52] Korobeinichev OP, Ermolin NE, Chernov AA, Emel'yanov ID. Flame structure, kinetics, and mechanism of chemical reactions in flames of mixed composition based on ammonium perchlorate and polybutadiene rubber. Combustion, Explosion, and Shockwaves 1992;28(4):366–71.
[53] Volkov EN, Paletsky AA, Korobeinichev OP. RDX flame structure at atmospheric pressure. Combustion, Explosion, and Shockwaves 2008;44:43–54.
[54] Chorpening BT, Knott GM, Brewster MQ. Flame structure and burning rate of ammonium perchlorate/hydroxyl-terminated polybutadiene propellant sandwiches. Proc Combustion Inst 2000;28:847–53.
[55] Fitzgerald RP, Brewster MQ. AP/HTPB laminate propellant flame structure: Fuel-lean intrinsic instability. Proc Combust Inst 2007;31:2071–8.
[56] Fitzgerald RP, Brewster MQ. Infrared imaging of AP/HTPB laminate propellant flames. Combust Flame 2008;154:660–70.
[57] Jojic I, Brewster MQ. Condensed-phase chemical interaction between ammonium perchlorate and hydroxy-terminated polybutadiene. J Propul Power 1998;14(4):575–6.
[58] Weiser V, Eisenreich N, Baier A, Eckl W. Burning behavior of ADN formulations. Propellants Explos Pyrotech 1999;24:163–7.
[59] Yang R, Li Y, Zhang J, Zhu S, Fang Z, Li Y, et al. Diagnostics of flame temperature distribution of solid propellants by spectrographic analysis. Combust Flame 2006;145:836–44.
[60] Demtröder W. Laser spectroscopy, Volume 1: Basic principles. Heidelberg: Springer-Verlag, Berlin; 2008.
[61] Homan BE, Vanderhoff JA. Absorption spectroscopy of RDX monopropellant flames: CN and NH concentrations. In: Proceedings of SPIE 3172, Optical technology in fluid, thermal, and combustion flow III, 1997.
[62] Wormhoudt J, Kebabian PL, Kolb CE. Infrared fiber-optic diagnostic observations of solid propellant combustion. Combust Flame 1997;108:43–60.
[63] Lu YC, Freyman T, Kuo KK. Measurements of temperatures and OH concentrations of solid propellant flames using absorption spectroscopy. Combust Sci Technol 1995;104(1):193–205.
[64] Kim ES, Lee HS, Mallery CF, Thynell ST. Thermal decomposition studies of energetic materials using confined rapid thermolysis/FTIR spectroscopy. Combust Flame 1997;110:239–55.
[65] Li Y, Wang J. The real time diagnostics of combustion characteristics of solid propellant by remote sensing FTIR system. Instrum Sci Technol 2003;31(1):33–45.
[66] Smooke M, Yetter R, Parr T, Hanson-Parr D. Experimental and modeling studies of two-dimensional ammonium perchlorate diffusion flames. Proc. Combust. Inst. 2000;28:839–46.
[67] Hedman TD, Cho KY, Satija A, Groven LJ, Lucht RP, Son SF. Experimental observation of the flame structure of a bimodal ammonium perchlorate composite propellant using 5 kHz PLIF. Combust Flame 2012;159:427–37.
[68] Parr T, Hanson-Parr D. RDX/GAP/BTTN propellant flame studies. Combust Flame 2001;127:1895–905.
[69] Parr T, Hanson-Parr D. Cyclotetramethylene tetranitramine/glycidyl azide polymer/butanetriol trinitrate propellant flame structure. Combust Flame 2004;137:38–49.
[70] Stufflebeam JH, Eckbreth AC. CARS diagnostics of solid propellant combustion at elevated pressure. Combust Sci Technol 1989;66:163–79.
[71] Kearney SP, Guildenbecher DR. Temperature measurements in metalized propellant combustion using hybrid fs/ps coherent anti-Stokes Raman scattering. Appl Opt 2016;55(18):4958–66.
[72] O'Neil M, Niemiec NA, Demko A, Peterson EL, Kulatilaka WD. Laser-induced-breakdown-spectroscopy-based detection of metal particles released into the air during combustion of solid propellants. Appl Opt 2018;57(8):1910–7.
[73] Beckstead M. Combustion calculations for composite solid propellants. In: JANNAF combustion meeting, Monterey, 1976.
[74] Beckstead M. A model for solid propellant combustion. In: JANNAF Combustion Meeting, Colorado Springs, 1977.
[75] Hermance C. A model of composite propellant combustion including surface heterogeneity and heat generation. AIAA J 1966;4(9):1629–37.
[76] Maurer M, Bojko BT, Byrd EFC, Kalman J. Ray tracing calculations in simulated propellant flames with detailed chemistry. Appl Opt 2019;58(6):1451–9.
[77] Strunin V, Manelis G, Ponomarev A, Tal'roze V. Effect of ionizing radiation on the combustion of ammonium perchlorate and composite systems based on ammonium perchlorate. Combustion, Explosion, and Shock Waves 1968;4(4):584–90.
[78] Manelis G, Strunin V. The mechanism of ammonium perchlorate burning. Combust Flame 1971;17:69–77.
[79] Strunin V, Firsov A, Shkadinskii K, Manelis G. Stationary combustion of decomposing and evaporating condensed substances. Fiz Goreniya Vzryva 1977;13(1):3–9.
[80] Price C, Boggs T, Jr. B, H.H., Modeling the combustion of monopropellants. In: JANNAF combustion meeting, Colorado Springs, 1977.
[81] Price C, Boggs T, Derr R. Modeling of solid monopropellant deflagration. In: AIAA 16th aerospace sciences meeting, Huntsville, 1978.
[82] Shusser M, Culick F, Cohen N. Combustion response of ammonium perchlorate. AIAA J 2002;40(4):722–30.
[83] Miller M. In search of an idealized model of homogeneous solid propellant combustion. Combust Flame 1982;46:51–73.
[84] Miller M, Coffee T. A fresh look at the classical approach to homogeneous solid propellant combustion modeling. Combust Flame 1983;50:65–74.
[85] Miller M, Coffee T. On the numerical accuracy of homogeneous solid propellant combustion models. Combust Flame 1983;50:75–88.
[86] Miller M, Coffee T, Kotlar A. The use of microthermocouples to measure temperature profiles in burning propellants. In: JANNAF combustion meeting, Laurel, 1985.
[87] Sahu H, Sheshadri T, Jain V. Novel kinetic scheme for the ammonium perchlorate gas phase. J Phys Chem 1990;94:294–5.
[88] Ramakrishna P, Paul P, Mukunda H. Revisiting the modeling of ammonium-perchlorate combustion: development of an unsteady model. J Propul Power 2006;22(3):661–8.
[89] Giovangigli V, Meynet N, Smooke M. Application of continuation techniques to ammonium perchlorate plane flames. Combust Theor Model 2006;10(5):771–98.
[90] Rahman S, Giovangigli V, Borie V. Pressure and initial temperature sensitivity coefficient calculations in ammonium perchlorate flames. J Propul Power 2011;27(5):1054–63.
[91] Vo N, Jung M, Oh D, Park J, Moon I, Oh M. Moving boundary modeling for solid propellant combustion. Combust Flame 2018;189:12–23.
[92] Jeppson M, Beckstead M, Jing Q. A kinetic model for the premixed combustion of a fine AP/HTPB composite propellant. In: AIAA Aerospace sciences meeting, Reno, 1997.
[93] Merzhanov A, Shteinberg A, Goncharov E. High-temperature decomposition of ammonium perchlorate and heterogeneous systems based on ammonium perchlorate. Fiz Goreniya Vzryva 1973;9(2):185–91.
[94] Cohen N, Strand L. An improved model for the combustion of AP composite propellants. AIAA J 1982;20(12):1739–46.
[95] Summerfield M, Sutherland G, Webb M, Taback H, Hall K. Burning mechanism of ammonium perchlorate propellants, ARS progress in astronautics and rocketry – Vol. 1: Solid propellant rocket research, vol. 1, pp. 141–182, 1960.
[96] Buckmaster J, Jackson T, Yao J. An elementary discussion of propellant flame geometry. Combust Flame 1999;117:541–52.
[97] Jackson T, Buckmaster J. Nonpremixed periodic flames supported by heterogeneous propellants. J Propul Power 2000;16(3):498–504.
[98] Ermolin N, Korobeinichev O, Tereshchenko A, Fomin V. Measurement of the concentration profiles of reacting components and temperature in an ammonium perchlorate flame. Fizika Goreniya i Vzrva 1982;18(1):46–9.
[99] Ermolin N, Korobeinichev O, Tereshchenko A, Fomin V. Kinetic calculations and mechanism definition for reactions in an ammonium perchlorate flame. Fiz Goreniya Vzryva 1982;18(2):61–70.
[100] Ermolin N, Korobeinichev O, Fomin V. On the kinetic mechanism of the reaction of NH2 with O2 in O-, H-, and N-containing flames. 1. Kinetic parameters of the NH2 + O2 = HNO + OH reaction. Fiz Goreniya Vzryva 1994;30(1):60–5.
[101] Ermolin N, Korobeinichev O, Fomin V. Kinetic mechanism of the reaction of NH2 with O2 in O-, H-, and N-containing flames. II. Estimation of kinetic parameters of the stages involving NH2O2, HNOOH, and NH2O. Fiz Goreniya Vzryva 1994;30(3):41–9.
[102] Ermolin N. Model for chemical reaction kinetics in perchloric acid-ammonia flames. Combustion, Explosion, and Shock Waves 1995;31(5):555–65.
[103] Smith G, Golden D, Frenklach M, Moriarty N, Eiteneer B, Goldenberg M, Bowman C, Hanson R, Song S, Gardiner Jr. W, Lissianski V, Qin Z. GRI-Mech 3.0, [Online]. Available: http://www.me.berkeley.edu/gri_mech/. [Accessed 30 10 2018].
[104] Smooke M, Yetter R, Parr T, Hanson-Parr D, Tanoff M, Colket M, Hall R. Computational and experimental study of ammonium perchlorate/ethylene counterflow diffusion flames. Proc Combust Inst 2000;28:2013–20.
[105] Gross M, Beckstead M. Diffusion flame calculations for composite propellants using a vorticity-velocity formulation. J Propul Power 2009;25(1):74–82.
[106] Gross M, Beckstead M. Steady-state combustion mechanisms of ammonium perchlorate composite propellants. J Propul Power 2011;27(5):1064–78.
[107] M. Nusca, Computational fluid dynamics model of laminate AP/HTPB propellant strands: Finite-rate chemical kinetics and AP particle size effects on burnrate at high pressure. In: JANNAF combustion meeting, Newport News, 2016.

[108] Nusca M. Computational fluid dynamics model of laminate AP/HTPB strands: AP particle size effect on burnrate at high pressure. In: JANNAF combustion meeting, Newport News, 2017.
[109] Chen C-C, McQuaid M. A skeletal, gas-phase, finite-rate, chemical kinetics mechanism for modeling the deflagration of ammonium perchlorate – hydroxyl-terminated polybutadiene composite propellants, ARL-TR-7655, Aberdeen Proving Grounds, 2016.
[110] Chen C-C, McQuaid M. Thermochemical and kinetics modeling pertaining to AP-HTPB composite propellant combustion. In: JANNAF propellant and explosives development, Salt Lake City, 2015.
[111] Miccio F. Numerical modeling of composite propellant combustion. Proc Combust Inst 1998:2387–95.
[112] Knott G, Brewster M. Two-dimensional combustion modeling of heterogeneous solid propellants with finite Peclet number. Combust Flame 2000;121:91–106.
[113] Zhou X, Jackson T, Buckmaster J. A numerical study of periodic sandwich propellants with oxygenated binders. Combust Theor Model 2003;7:435–48.
[114] Ramakrishna P, Paul P, Mukunda H, Sohn C. Combustion of sandwich propellant at low pressures. Proc Combust Inst 2005;30:2097–104.
[115] Hegab A, Jackson T, Buckmaster J, Stewart D. Nonsteady burning of periodic sandwich propellants with complete coupling between the solid and gas phases. Combust Flame 2001;125:1055–70.
[116] Hegab A, Sait H, Hussain A, Said A. Numerical modeling for the combustion of simulated solid rocket motor propellant. Comput Fluids 2014;89:29–37.
[117] Ramakrishna P, Paul P, Mukunda H. Sandwich propellant combustion: modeling and experimental comparison. Proc Combust Inst 2002;29:2963–73.
[118] Gross M, Hedman T, Son S, Jackson T, Beckstead M. Coupling micro and meso-scale combustion models of AP/HTPB propellants. Combust Flame 2013;160:982–92.
[119] Gaduparthi T, Pandey M, Chakravarthy S. Gas phase flame structure of solid propellant sandwiches with different reaction mechanisms. Combust Flame 2016;164:10–21.
[120] Navaneethan M, Srinivas V, Chakravarthy S. Coupling of leading edge flames in the combustion zone of composite solid propellants. Combust Flame 2008;153:574–92.
[121] Jackson TL, Buckmaster J, Hoeflinger J. Three-dimensional flames supported by heterogeneous propellants. Proc Combust Inst 2000;28(1):895–902.
[122] Knott G, Jackson T, Buckmaster J. Random packing of heterogeneous propellants. AIAA J 2001;39(4):678–86.
[123] Jackson T, Buckmaster J. Heterogeneous propellant combustion. AIAA J 2002;40(6):1122–30.
[124] Massa L, Jackson T, Short M. Numerical solution of three-dimensional heterogeneous solid propellants. Combust Theor Model 2003;7:579–602.
[125] Rajoriya G, Vijay C, Ramakrishna P. Thermal conductivity estimation of high solid loading particulate composites: a numerical approach. Int J Therm Sci 2018;127:252–65.
[126] Wang X, Buckmaster J, Jackson T. Burning of ammonium-perchlorate ellipses and spheroids in fuel binder. J Propul Power 2006;22(4):764–8.
[127] Plaud M, Gallier S, Morel M. Simulations of heterogeneous propellant combustion: Effect of particle orientation and shape. Proc Combust Inst 2015;25:2447–54.
[128] Murphy J, Krier H. Heterogeneous effects on dynamic burning in composite solid propellants. Proc Combust Inst 2000;28:885–93.
[129] Gusachenko L, Zarko V. Combustion models for energetic materials with completely gaseous reaction products. Combustion, Explosion, and Shock Waves 2005;41(1):20–34.
[130] Wang X, Jackson T, Massa L. Numerical simulation of heterogeneous propellant combustion by a level set method. Combust Theor Model 2004;8:227–54.
[131] Wang X, Hossain K, Jackson T. The three-dimensional numerical simulation of aluminized composite solid propellant combustion. Combust Theor Model 2008;12(1):45–71.
[132] Cazan R, Menon S. Direct numerical simulation of sandwich and random-packed propellant combustion. In: 39th AIAA joint propulsion meeting, Huntsville, 2003.
[133] Choi J, Cakmak M, Menon S. Simulations of composite solid propellant combustion using adaptive mesh refinement. In: 49th AIAA aerospace sciences meeting, Orlando, 2011.
[134] Surzhikov S, Krier H. Unsteady dynamic variables method for heterogeneous solid propellant burning. AIAA J 2001;39(12):2343–50.
[135] Favale G, Miccio F. Modeling unsteady and perturbed combustion of heterogeneous composite propellants. Aerosp Sci Technol 2008;12:285–94.
[136] Buckmaster J, Jackson T. The effects of time-periodic shear on a diffusion flame anchored to a propellant. Combust Flame 2000;120:211–21.
[137] Topalian V, Zhang J, Jackson T, Isfahani A. Numerical study of erosive burning in multidimensional solid propellant modeling. J Propul Power 2011;27(4):811–2.
[138] Massa L, Jackson T, Buckmaster J. Using heterogeneous propellant burning simulations as subgrid components of rocket simulations. AIAA J 2004;42(9):1889–900.
[139] Cai W, Thakre P, Yang V. A model of AP/HTPB composite propellant combustion in rocket-motor environments. Combust Sci Technol 2008;180:2143–69.
[140] McDonald B, Menon S. Direct numerical simulation of solid propellant combustion in crossflow. J Propul Power 2005;21(3):460–9.
[141] Isfahani A, Zhang J, Jackson T. The effects of turbulence-induced time-periodic shear on a flame anchored to a propellant. Combust Flame 2009;156:1084–98.
[142] Cao Y, Yu Y, Ye R. Numerical analysis of AP/HTPB composite propellant combustion under rapid depressurization. Appl Therm Eng 2015;75:145–53.
[143] Gallier S, Ferrand A, Plaud M. Three-dimensional simulations of ignition of composite solid propellants. Combust Flame 2016;173:2–15.
[144] Massa L, Jackson T. Multidimensional numerical simulation of ammonium-perchlorate-based propellant combustion with fine/ultrafine aluminum. J Propul Power 2008;24(2):161–74.
[145] Yan A, Son S, Jackson T, Venugopal P. Validation of numerical simulations for nano-aluminum composite solid propellants. J Propul Power 2011;27(6):1280–7.
[146] Beckstead M, Puduppakkam K, Thakre P, Yang V. Modeling of combustion and ignition of solid-propellant ingredients. Prog Energy Combust Sci 2007;33:497–551.
[147] Jackson T. Modeling of Heterogeneous Propellant Combustion: A Survey. AIAA Journal 2012;50(5):993–1006.
[148] Almodovar CA, Salazar D, Strand CL, Hanson RK, Wright RG, Brophy CM. TDLAS measurements of the underexpanded exhaust plume from a solid propellant gas generator. In: AIAA Scitech Forum, San Diego, CA, 2019.